The risk management approach to macro-prudential policy*

Sulkhan Chavleishvili,[(a)] *Robert F. Engle,*[(b)] *Stephan Fahr,*[(c)] *Manfred Kremer,*[(c)] *Frederik Lund-Thomsen,*[(c)] *Simone Manganelli,*[(c)] *Bernd Schwaab*[(c)]

[(a)] Aarhus University, [(b)] NYU Stern School of Business, [(c)] European Central Bank

March 4, 2024

Abstract

Macro-prudential authorities are tasked with assessing medium-term downside risks to the real economy stemming from financial imbalances and the associated threat of a future financial crisis. Before implementing policy measures to manage financial vulnerabilities, however, these authorities must also weigh the policies' potential cost in terms of the economy's upside potential. This setting gives rise to a risk management problem, a trade-off between limiting downside risks and preserving upside potential. We formalize the decision problem under uncertainty and study it for the euro area. Flexible and potentially asymmetric predictive distributions are obtained from a Bayesian structural quantile vector autoregressive model. We study the macro-prudential policy stance and evaluate the circumstances under which macro-prudential interventions are likely to yield beneficial outcomes.

Keywords: Growth-at-risk, structural quantile vector autoregression, Bayesian inference, financial conditions, macro-prudential policy.

JEL classification: G21, C33.

*We would like to thank Massimiliano Marcellino and Ivan Petrella for their helpful comments, as well as Jacopo Maria D'Andria, Albert Pierres Tejada, and Paul Delatte for excellent research support. E-mail contacts: sulkhan.chavleishvili@econ.au.dk; rengle@stern.nyu.edu; stephan.fahr@ecb.europa.eu; manfred.kremer@ecb.europa.eu; frederik_ole.lund-thomsen@ecb.europa.eu; simone.manganelli@ecb.europa.eu; bernd.schwaab@ecb.europa.eu (corresponding author). The views expressed in this paper are those of the authors and they do not necessarily reflect the views or policies of the European Central Bank.

1 Introduction

The Global Financial Crisis (GFC) of 2008–2009 underscored the critical need for robust macro-prudential policies. It became evident that monitoring the soundness of individual financial institutions was insufficient, and that the resilience of the entire financial system needed to be taken into account; see e.g. the reports by Brunnermeier et al., 2009 and de Larosiere, 2009. The severity of the GFC exposed a pronounced underestimation of medium-term downside risks to the economy resulting from a gradual accumulation of financial vulnerabilities. A plethora of theoretical and empirical frameworks have since been developed to assess and manage downside risks, including, for example, Brunnermeier and Sannikov, 2014, Boissay et al., 2016, He and Krishnamurthy, 2019, Adrian et al., 2019, Suarez, 2021, Caldara et al., 2021, and Carriero et al., 2023. Yet, effective macro-prudential policies cannot focus solely on mitigating downside risks, but must balance risk mitigation with growth considerations. As former UK Chancellor George Osborne aptly put it, *"we do not want the financial stability of a graveyard."* How to formalize this key trade-off as an economic decision problem under uncertainty, and how to study it empirically for an advanced market-based economy, however, is currently unclear. This is despite a formal framework's obvious theoretical appeal and macro-prudential policymakers' urgent need for analytical support.

This paper develops a comprehensive framework to formalize the decision problem faced by the macro-prudential authority, and applies it to the euro area. To our knowledge, we are the first to extend the "risk management" approach of Greenspan (2003, p. 3), Cecchetti (2006), and Kilian and Manganelli (2008) to address the macro-prudential problem, and to use a flexible but fully tractable semi-parametric structural quantile vector autoregressive (SQVAR) model to bring the approach to life. While, strictly speaking, SQVAR models are not new (Chavleishvili and Manganelli, 2023), the SQVAR framework in this paper is novel in considering more than two variables at more than one lag, allowing for exogenous global variables, and proposing a coherent Bayesian (rather than frequentist) inference methodology for its statistical analysis. Whenever possible, we relate our empirical results to models of financial frictions or other macroeconomic models.

Current measures of economic downside risk are borrowed from the financial risk management literature: Growth-at-Risk (GaR) is Value-at-Risk (VaR) applied to the gross domestic product (GDP) instead of a bank's investment portfolio (Adrian et al., 2019, Adrian et al., 2022). GaR is the tail quantile (usually 5%) of the variable of interest. The main advantage of GaR is its simplicity: by definition, GDP growth will not be below the estimated GaR with 95% probability. However, this type of measure has been criticized in the financial econometrics literature on the grounds that it does not take the whole tail of the distribution into account, as well as for not being a coherent (e.g. sub-additive) measure of risk. More importantly, it captures only one part (the downside) of the macro-prudential decision problem, and is silent on the upside potential for the economy.

We address the limitations of GaR by introducing *growth shortfall* as a measure of downside risk, and by complementing it with *growth longrise* to gauge the economy's upside potential. Growth shortfall (longrise) is the scaled growth expectation, conditional on realizing a value below (above) a certain threshold. Zero serves as a natural threshold when applied to GDP growth, distinguishing economic contractions from expansions. By design, the sum of growth shortfall and longrise equals the expected growth. If the macro-prudential authority assigns equal importance to both components, its goal would be to just maximize expected growth. However, the policymaker's objective is to prevent severe and painful economic contractions without unnecessarily limiting growth potential. The decision framework proposed in this paper formalizes this trade-off by assigning greater weight to growth shortfall than to longrise.

We illustrate our decision framework by implementing it for the euro area. The empirical implementation necessitates estimating the joint predictive distribution of all macroeconomic variables of interest.[1] We recover flexible, and potentially asymmetric predictive distributions using a

[1]Because of the asymmetric emphasis on downside risk, expected growth is no longer a sufficient statistic to solve the macro-prudential risk management problem. In principle, the mean could still be a sufficient statistic if the random variables of interest were symmetric and with time-invariant higher moments. In such a case, estimates of the conditional means of the random variables of interest, augmented by suitable assumptions of the distribution of the residuals, would suffice. However, there is by now substantial empirical evidence that financial variables exert a time-varying and asymmetric impact on real variables (see, e.g., Adrian et al., 2019, Delle Monache et al., 2023, and Iseringhausen et al., 2024). This necessitates the use of suitable econometric models that account for these characteristics.

semi-parametric SQVAR model. SQVAR extends the concept of structural VAR to quantile modeling. Essentially, while VARs model the *mean* dynamic interaction of the endogenous variables of a system, QVARs model the dynamic interaction of any *quantile* of the variables of interest. Structural identification is obtained by standard recursive modeling. Once the model is estimated for all quantiles, estimates of all predictive distributions can be obtained by sampling from the estimated quantiles; the main text and web appendix provide the necessary details.

We estimate the SQVAR model's parameters using Bayesian methods. We rely on established methodology (Yu and Moyeed, 2001, Kozumi and Kobayashi, 2011, Khare and Hobert, 2012), but also make an econometric contribution. Leveraging the Bayesian approach, our estimates of the euro area parameters depend on an informative prior density to sharpen inference, which we obtain from a different but related sample (several decades of United States (U.S.) data). That is, we first obtain posterior estimates from U.S. data, which then serve as informative priors for the euro area parameters. The prior variance, which represents the "weight" assigned to the prior density, can be estimated from the euro area data following the Empirical Bayes approach of Giannone et al. (2015). Doing so extends the three-step Gibbs sampler of Khare and Hobert (2012) to four steps. Overall, our approach to inference allows us to obtain precise posterior estimates of measures of downside risk and upside potential, among other nonlinear functions of the model's deterministic parameters. In addition, we obtain appropriate finite-sample credible intervals, despite a relative paucity of euro area quarterly macro data and a moderate-to-large number of parameters to be estimated in each equation of the SQVAR (Chernozhukov and Fernandez-Val, 2011).

Our preferred SQVAR model includes a measure of the financial cycle, real GDP growth, HICP inflation, financial stress, and a short-term risk-free interest rate and uses four lags. Its parameters are estimated from euro area data between 1990Q1 and 2022Q4. A global commodity price index is included as an additional exogenous variable to help explain time variation in inflation and real GDP. The financial cycle is a measure of credit dynamics in the economy and represents an intermediate target variable on which macro-prudential policymakers can act by activating or adjusting macro-prudential instruments. Financial stress characterizes financial crises and can

amplify other shocks (e.g., He and Krishnamurthy, 2019). Overall, our choice of variables reflects the idea that financial stability is of concern to policymakers if it is triggered by an impairment of the financial system and has real economic consequences, e.g. in terms of future economic activity.[2] The monetary part of the system (with inflation and interest rate) is included to take the impact of the central bank's actions into account.

We highlight four empirical results.

First, the estimated SQVAR is characterized by substantial asymmetries, in the sense that the dynamic properties of the system differ considerably across quantiles. For example, a shock to financial stress shifts the left tail of future GDP growth outward, while leaving its conditional median and right tail approximately unaffected. These macro-financial interactions imply that the upper quantiles of the predictive GDP growth distribution are considerably less volatile than its lower quantiles. This result is in line with Adrian et al. (2019) and Adrian et al. (2022). It also lends empirical support to macroeconomic models that allow for asymmetric impacts of financial variables on macroeconomic outcomes, including, for example, nonlinear macro-financial models with occasionally binding financing constraints such as He and Krishnamurthy (2019), Van der Ghote (2021), and Mendicino et al. (2024).

Second, our model-implied downside risk estimates are sensitive to the inclusion of financial variables. In a model specification with only own lags of real GDP growth, and thus without financial variables, estimates of downside risks pertaining to the GFC only respond as the crisis happens, and less forcefully so, while the 2010–2012 euro area sovereign debt crisis is missed almost entirely. This result lends support to GaR models that include financial conditions as explanatory variables, such as Adrian et al. (2019) and Adrian et al. (2022), and lends less support to the notion that autoregressive terms and the now-casting of macroeconomic conditions are key and necessary features (Plagborg-Moller et al., 2020).

[2]The ECB definition of financial stability refers to *"the risk that the provision of necessary financial products and services by the financial system will be impaired to a point where economic growth and welfare may be materially affected;"* see ECB (2019). Similarly, the Financial Stability Board, International Monetary Fund, and the Bank for International Settlements define systemic risk as a *"risk of disruption to financial services that is (i) caused by an impairment of all or parts of the financial system, and (ii) has the potential to have serious negative consequences for the real economy;"* see FSB (2009).

Third, the outcomes of model-based stress tests suggest that the resilience of the euro area economy to a sequence of adverse financial shocks is not constant over time.[3] Our results indicate that downside risk measures, conditional on future adverse financial shocks, tend to climb in the lead-up to a crisis, during which they then spike. These risks were most pronounced in the aftermath of the GFC and the euro area sovereign debt crisis. Moreover, the impact of an initial shock to financial stress is not solely dependent on its initial severity, but also hinges on the endogenous, asymmetric responses of all other variables in the system, as e.g. suggested by He and Krishnamurthy (2019), Van der Ghote (2021), and Mendicino et al. (2024). Overall, the pronounced economic asymmetries revealed in the data suggest that our semi-parametric modeling framework could be well-suited for conducting repeated model-based stress tests of the entire macro-financial system.

Finally, our framework provides a metric to assess whether the macro-prudential stance is too tight or too loose. Welfare calculations for leaning against an exuberant financial cycle can be based on an appropriate objective function that weights growth shortfall and longrise differently. We find that the associated welfare gains can be positive or negative. Historically, the gains from macro-prudential policy tightening tended to be positive in economic expansions and negative in contractions. This suggests that macro-prudential policymakers should act in a counter-cyclical fashion by releasing buffers when downside risk is exceptionally high and increasing them gradually over time when downside risks are low or moderate (see also Van der Ghote, 2021).

Our work is related to at least two strands of the literature. First, a rapidly growing body of research has examined downside risk in macroeconomic outcomes. Most of this work has focused on the risk of considerable declines in real GDP, brought about by a deterioration of financial conditions; see e.g. Adrian et al. (2019), Prasad et al. (2019), and Caldara et al. (2021). In particular, the International Monetary Fund (IMF), the European Central Bank (ECB), and the Federal Reserve Bank of New York now routinely publish GaR estimates for major world economies; see IMF (2017), ECB (2019), and New York Fed (2022). These developments have motivated a pro-

[3] We define stress testing as a density forecast of the potential impact on all variables in the system when subjected to a certain sequence of adverse shocks.

liferation of modeling frameworks to assess the severity of extreme events associated with key economic variables, including single-equation QR models (Adrian et al., 2019), panel QR models (Brandao-Marques et al., 2020, Adrian et al., 2022), panel-GARCH models (Brownlees and Souza, 2020), fully non-parametric kernel regression models (Adrian et al., 2021), combined linear vector autoregressive (VAR) and single-equation QR models (Duprey and Ueberfeldt, 2020, Forni et al., 2021), nonlinear Bayesian VAR models (Caldara et al., 2021, Carriero et al., 2023), and quantile FAVAR models (Korobilis and Schröder, 2023). De Santis and van der Veken (2020) show that even if a recession is due to an unforeseen real shock (such as the 2020 Covid-19 recession), financial variables can still provide policymakers with timely warnings about the severity of the crisis and the macroeconomic risks involved.

Second, the SQVAR model relates to the single-equation quantile regression (QR) approach of Adrian et al. (2019) as the VAR model of Sims (1980) relates to the earlier single-equation AR approaches of e.g. Koyck (1954) and Almon (1965). To our knowledge, QVAR was first proposed in unpublished work by Cecchetti and Li (2008). White et al. (2015), Chavleishvili and Manganelli (2023), Iacopini et al. (2023), and Iacopini et al. (2024) contributed to formalizing the econometric model. These works fit into the broader literature on multivariate QR, which is an active area of research (see, for instance, Wei, 2008, Carlier et al., 2016, and Iacopini et al., 2024).

We proceed as follows. Section 2 defines downside risk measures and presents our decision framework. Section 3 introduces the statistical model. Section 4 describes the euro area data. Section 5 discusses our key empirical results. Section 6 concludes. A web appendix provides further technical and empirical results.

2 The risk management decision framework

This section first defines three measures of downside risk and two measures of upside potential. Some of these measures are related to well-known concepts from the financial risk management literature. It then integrates these measures into an encompassing decision framework.

2.1 Measures of downside risk

2.1.1 Growth-at-risk

Our first measure of adverse impact is *growth-at-risk* ($\text{GaR}^{\gamma}_{t,t+h}$) at confidence level $\gamma \in (0,1)$, defined implicitly by the probability

$$\mathbb{P}\left[y_{t+h} \leq \text{GaR}^{\gamma}_{t,t+h} | \Omega_{1t}\right] = \gamma, \tag{1}$$

where y_t is the quarterly annualized real GDP growth rate between time $t-1$ and t, $h = 1, \ldots, H$, and H is a certain prediction horizon. The information set Ω_{1t} contains all data known at time t; see Section 3. In words, $\text{GaR}^{\gamma}_{t,t+h}$ is implicitly defined by the time t probability of quarterly annualized output growth at $t+h$ falling below $\text{GaR}^{\gamma}_{t,t+h}$, which by definition is set equal to γ (see, for example, McNeil et al., 2005, Ch. 2.2).

2.1.2 An expectation-based risk measure: growth shortfall

Our second measure of adverse real economic impact is *growth shortfall* (GS), defined as

$$\begin{aligned} \text{GS}^{\tau}_{t,t+h} &= \int_{-\infty}^{\tau} y_{t+h} dF_{t,t+h}(y_{t+h}) \\ &= \mathbb{E}\left[y_{t+h} | y_{t+h} < \tau, \Omega_{1t}\right] \times \mathbb{P}\left[y_{t+h} < \tau | \Omega_{1t}\right], \end{aligned} \tag{2}$$

where $F_{t,t+h}$ is a time-t conditional cdf, $\mathbb{E}\left[\cdot|\Omega_{1t}\right]$ denotes a time-t conditional expectation, and the threshold $\tau \in \mathbb{R}$ could be set to a low conditional quantile, say $\tau = \text{GaR}^{\gamma}_{t,t+h}$. If so, then the first factor in (2) coincides with the familiar notion of expected shortfall; see e.g. McNeil et al. (2005, Ch. 2). Alternatively, it could be set to a certain unconditional quantile, or to zero. In this case, the first factor in (2) does *not* coincide with expected shortfall from the financial risk management literature.

If $\tau = 0$, GS can be factored into two intuitive terms: the expected loss conditional on a

contraction, and the probability of experiencing a contraction.[4] While both components could, in principle, be studied separately and be of interest in their own right, GS summarizes them tractably into one metric. When $\tau = 0$, GS corresponds to the economic question: what is the time t-expected contraction of the economy at time $t + h$.

A straightforward and final measure of adverse real economic impact is the *average future growth shortfall* (AGS) between $t + 1$ and $t + H$, defined as

$$\text{AGS}^{\tau}_{t,t+1:t+H} = H^{-1} \sum_{h=1}^{H} \text{GS}^{\tau}_{t,t+h}. \tag{3}$$

If $\tau = 0$, then the AGS corresponds to the question: what is the average future expected contraction of the economy between $t + 1$ and $t + H$.

All the above risk measures are economically intuitive and straightforward to communicate. Risk measures (2) and (3), however, have theoretical and practical advantages over (1). First, while all above risk measures (1) – (3) can take into account the asymmetric impact of financial variables on the economy, only (2) and (3) take into account the entire left tail. Second, (scaled) expected shortfall is a coherent risk measure, while any single quantile in isolation is not (Artzner et al., 1999). For example, growth shortfall contributions are sub-additive, while GaR contributions are not. This feature is desirable if one, for instance, sought to study sector contributions to aggregate GDP-at-risk.

2.2 Measures of upside potential: growth longrise

When considering financial stability policies aimed at containing downside risk, the upper quantiles of future GDP growth, should, ideally, not be negatively affected. For setting up the decision framework in Section 2.3, we consider two measures of upside potential that are symmetric to two measures of downside risk just defined.

[4] To see this, note that $\mathbb{E}\left[y_{t+h} | y_{t+h} < \tau, \Omega_{1t}\right] \equiv \frac{\int_{-\infty}^{\infty} y_{t+h} \cdot 1\{y_{t+h} < \tau\} dF_{t,t+h}(y_{t+h})}{\int_{-\infty}^{\infty} 1\{y_{t+h} < \tau\} dF_{t,t+h}(y_{t+h})} = \frac{\int_{-\infty}^{\tau} y_{t+h} dF_{t,t+h}(y_{t+h})}{\mathbb{P}[y_{t+h} < \tau | \Omega_{1t}]}$.

First, we define the *growth longrise* (GL) as the complement to GS,

$$\begin{aligned}\text{GL}^{\tau}_{t,t+h} &= \int_{\tau}^{\infty} y_{t+h} dF_{t,t+h}(y_{t+h}) \\ &= \mathbb{E}\left[y_{t+h} | y_{t+h} > \tau, \Omega_{1t}\right] \times \mathbb{P}\left[y_{t+h} > \tau | \Omega_{1t}\right]. \end{aligned} \tag{4}$$

If $\tau = 0$, then (4) corresponds to the question: what is the time-t expected expansion of the economy between $t+h-1$ and $t+h$? Similarly to GS, the growth longrise (4) captures the expected growth given an expansion, and the conditional probability of experiencing an expansion.[5] Given the complementarity between GS and GL, their sum equals the expected growth rate of the economy between $t+h-1$ and $t+h$,

$$\begin{aligned}\mathbb{E}\left[y_{t+h} | \Omega_{1t}\right] &= \int_{-\infty}^{\infty} y_{t+h} dF_{t,t+h}(y_{t+h}) \\ &= \int_{-\infty}^{\tau} y_{t+h} dF_{t,t+h}(y_{t+h}) + \int_{\tau}^{\infty} y_{t+h} dF_{t,t+h}(y_{t+h}) = \text{GS}^{\tau}_{t,t+h} + \text{GL}^{\tau}_{t,t+h}.\end{aligned}$$

Second, and analogously to (3), the *average growth longrise* (AGL) between $t+1$ and $t+H$ is

$$\text{AGL}^{\tau}_{t,t+1:t+H} = H^{-1} \sum_{h=1}^{H} \text{GL}^{\tau}_{t,t+h}. \tag{5}$$

For later reference, we note that $\text{AGS}^{\tau}_{t,t+1:t+H} + \text{AGL}^{\tau}_{t,t+1:t+H} = \mathbb{E}\left[\bar{y}_{t+1:t+H} | \Omega_{1t}\right]$, where $\bar{y}_{t+1:t+H}$ is the average future growth rate of the economy H quarters ahead. As a result, time-t expected growth can be read off any figure reporting $\text{AGS}^{\tau}_{t,t+1:t+H}$ and $\text{AGL}^{\tau}_{t,t+1:t+H}$ by adding the two lines.

2.3 Putting it all together in a risk management framework

A key question for a policymaker is to what extent a policy intervention reduces downside risk to the economy and what risk it imposes in terms of reduced upside potential. Specifically, how can a policymaker assess the change in forecast distributions triggered by her actions? We address

[5] To our knowledge, the term "longrise" was coined by Adrian et al. (2019) as the antonym to "shortfall."

this question by requiring the policymaker to be explicit about the trade-off between mitigating downside risks and preserving upside potential. It is equivalent to requiring the decision maker to provide a utility function and to set policy variables to maximize it.

Suppose the macro-prudential authority has a macro-prudential instrument m_t (or vector of instruments, including a Basel III counter-cyclical capital buffer) that can be used to mitigate medium-term downside risks to the economy by influencing the financial cycle $c_t(m_t)$. The influence of the financial cycle on the economy's predictive growth distribution can be direct $\big(c_t(m_t) \to y_{t+h}\big)$, or indirect via its impact on other variables, such as financial stress $\big(c_t(m_t) \to s_{t+h} \to y_{t+h}\big)$. The SQVAR structure allows us to capture both types of transmission. A convenient way to penalize downside risk is given by specifying the utility maximization problem as

$$\max_{\{m_{t+h}\}_{h=1}^{\infty}} \sum_{h=1}^{\infty} \delta^h \Big[GL_{t,t+h}\big(y_{t+h}(c_{t:t+h}(m_{t:t+h}))\big) + \lambda^p GS_{t,t+h}\big(y_{t+h}(c_{t:t+h}(m_{t:t+h}))\big) \Big] \tag{6}$$

where $\lambda^p > 1$ is a weight determining the policymaker's aversion to negative realizations of output growth, $0 < \delta \leq 1$ is an intertemporal discount factor, $m_{t:t+h} = (m_t, \ldots, m_{t+h})'$, $c_{t:t+h} = (c_t, \ldots, c_{t+h})'$, and $GS_{t,t+h}$ is always a negative number for $\tau \leq 0$.

Since $\text{GS}^{\tau}_{t,t+h}$ and $\text{GL}^{\tau}_{t,t+h}$ add to expected growth $\mathbb{E}\left[y_{t+h}|\Omega_{1t}\right]$, see Section 2.2, the objective function (6) can be rewritten in terms of expected economic growth instead of growth longrise,

$$\max_{\{m_{t+h}\}_{h=1}^{\infty}} \sum_{h=1}^{\infty} \delta^h \Big[\mathbb{E}_t\big(y_{t+h}(c_{t:t+h}(m_{t:t+h}))\big) + (\lambda^p - 1) GS_{t,t+h}\big(y_{t+h}(c_{t:t+h}(m_{t:t+h}))\big) \Big], \tag{7}$$

trading off supporting expected growth against mitigating downside risks. The objective function (7) is close to an expression suggested in a speech by Carney (2020). We also refer to Suarez (2021) for a micro-foundation of a similar objective function based on a representative agent with a CARA utility function on GDP. We use (7) to study the benefits of adopting an active financial stability policy in Section 5.5 below.

3 Structural quantile vector autoregression

3.1 The statistical model

This section summarizes the structural quantile vector autoregressive model (SQVAR). We start by observing a series of random variables $\{x_t : t = 1, \ldots, T\}$, where $x_t \in \mathbb{R}^n$ is an n-vector with ith element denoted by x_{it} for $i = 1, \ldots, n$ and $n \in \mathbb{N}$. It is important to define a recursive information set, which allows us to work with the stratified modeling strategy suggested by Wei (2008) and adapted in Chavleishvili and Manganelli (2023).

Recursive information set — The recursive information set is defined as:

$$\begin{aligned}\Omega_{1t} &\equiv \{x_{t-1}, x_{t-2}, \ldots\} \\ \Omega_{it} &\equiv \{x_{i-1,t}, \Omega_{i-1,t}\} \quad i = 2, \ldots, n.\end{aligned}$$

According to this definition, the recursive information set Ω_{2t}, say, contains all the lagged values of x_t as well as the contemporaneous value of x_{1t}. We say that x_t follows a SQVAR(1) process if the recursive γ_i quantile of x_{it} can be written as

$$\begin{aligned}Q_{\gamma_1}(x_{1t}|\Omega_{1t}) &= \omega_1(\gamma_1) + a_{11}(\gamma_1)x_{1,t-1} + a_{12}(\gamma_1)x_{2,t-1} + \ldots + a_{1n}(\gamma_1)x_{n,t-1} \\ Q_{\gamma_2}(x_{2t}|\Omega_{2t}) &= \omega_2(\gamma_2) + a_{021}(\gamma_2)x_{1t} + \\ &\quad + a_{21}(\gamma_2)x_{1,t-1} + a_{22}(\gamma_2)x_{2,t-1} + \ldots + a_{2n}(\gamma_2)x_{n,t-1} \\ &\vdots \\ Q_{\gamma_n}(x_{nt}|\Omega_{nt}) &= \omega_n(\gamma_n) + a_{0n1}(\gamma_n)x_{1t} + \ldots + a_{0n,n-1}(\gamma_n)x_{n-1,t} + \\ &\quad + a_{n1}(\gamma_n)x_{1,t-1} + a_{n2}(\gamma_n)x_{2,t-1} + \ldots + a_{nn}(\gamma_n)x_{n,t-1}\end{aligned}$$

for any $\gamma_i \in (0, 1)$, $i \in \{1, \ldots, n\}$. When $n = 1$, this simplifies to the quantile autoregressive process of Koenker and Xiao (2006).

In compact notation, we write an SQVAR(p) process as

$$\underbrace{Q_\gamma(x_t|\Omega_t)}_{n\times 1} = \underbrace{\omega(\gamma)}_{n\times 1} + \underbrace{A_0(\gamma)}_{n\times n}\underbrace{x_t}_{n\times 1} + \sum_{j=1}^{p}\underbrace{A_j(\gamma)}_{n\times n}\underbrace{x_{t-j}}_{n\times 1}, \tag{8}$$

where $\gamma \equiv [\gamma_1, \ldots, \gamma_n]'$ and the other elements stack the appropriate terms. Here, the matrix $A_0(\gamma)$ is a lower-triangular $n \times n$ matrix, with zeros along the main diagonal. The $n \times n$ matrices $A_j(\gamma)$ for $j = 1, \ldots, p$ are unrestricted. In the context of the VAR literature, this representation is equivalent to identifying the system by assuming a Cholesky decomposition of the covariance matrix of the residuals from a standard reduced form VAR.

A brief example may be instructive. While our empirical model in Section 5 considers $n = 5$ variables, $q = 19$ quantiles, and $p = 4$ lags, we can consider a bivariate model for the data vector $x_t = (y_t, s_t)'$, where y_t is the quarterly annualized real GDP growth between $t-1$ and t, and s_t is a coincident indicator of systemic financial stress. In this much simpler model, we consider one lag ($p = 1$) and only two quantiles: 0.1 for GDP, and 0.9 for financial stress. The system (8) can then be written as

$$\begin{bmatrix} Q_{.1}(y_t|\Omega_{1t}) \\ Q_{.9}(s_t|\Omega_{2t}) \end{bmatrix} = \begin{bmatrix} \omega_1(.1) \\ \omega_2(.9) \end{bmatrix} + \begin{bmatrix} 0 & 0 \\ a_{021}(.9) & 0 \end{bmatrix} \begin{bmatrix} y_t \\ s_t \end{bmatrix} + \begin{bmatrix} a_{11}(.1) & a_{12}(.1) \\ a_{21}(.9) & a_{22}(.9) \end{bmatrix} \begin{bmatrix} y_{t-1} \\ s_{t-1} \end{bmatrix}.$$

We here note, in particular, the lower-triangular matrix A_0, the contemporaneous term $x_t = (y_t, s_t)'$ on the right-hand side, and that different quantiles can be considered for different variables. In this example, a shock to y_t moves the 0.9 quantile of s_t by $a_{021}(.9)$, and a shock to s_t moves the 0.1 quantile of y_{t+1} by $a_{12}(.1)$.

In addition to more endogenous variables x_t, a realistic SQVAR will often include multiple lags, deterministic terms d_t including dummy variables, and exogenous variables z_t. Specifically,

the SQVAR(p) studied in Section 5 will be of the form

$$\underbrace{Q_\gamma(x_t|\Omega_t)}_{n\times 1} = \underbrace{\omega(\gamma)}_{n\times 1} + \underbrace{A_0(\gamma)}_{n\times n}\underbrace{x_t}_{n\times 1} + \sum_{j=1}^{p}\underbrace{A_j(\gamma)}_{n\times n}\underbrace{x_{t-j}}_{n\times 1} + \underbrace{B(\gamma)}_{n\times k}\underbrace{d_t}_{k\times 1} + \sum_{j=0}^{p}\underbrace{C_j(\gamma)}_{n\times r}\underbrace{z_{t-j}}_{r\times 1}, \tag{9}$$

where k and r denote the number of included deterministic terms and exogenous variables, respectively. Exogenous variables z_t are modeled via univariate quantile autoregressions; see Web Appendices A.

3.2 Parameter estimation

We estimate the SQVAR parameters using Bayesian methods. Building heavily upon already-established methodology (Yu and Moyeed, 2001, Kozumi and Kobayashi, 2011, and Khare and Hobert, 2012) is possible since the lower-triangular structure on A_0 allows us to estimate the model parameters via $n \times q$ univariate quantile regressions, equation-by-equation.

We use informative priors to sharpen inference. Specifically, we first obtain parameter estimates from decades of U.S. data.[6] The U.S. parameters' posterior density is then used as an informative prior for the corresponding euro area model parameters. The weight put on the U.S. prior is estimated from euro area data, extending the three-step Gibbs sampler of Khare and Hobert (2012) to a novel four-step sampler. The additional step estimates a prior precision parameter by sampling from a known inverse-Gamma distribution. By using non-sample U.S. information in an Empirical Bayes way, we obtain appropriately precise posterior estimates for euro area parameters, downside risk measures, and quantile impulse response functions (see Section 3.4), along with appropriate finite-sample credible intervals, despite a relative paucity of euro area macro data and a considerable number of parameters to estimate. The difference between the U.S. and euro area estimates reflects the informational content of euro area data. Web Appendix A.1 discusses the four-step Gibbs sampler used for posterior inference. Web Appendix A.2 discusses prior specifications. Web Appendix A.3 derives the fourth step of the Gibbs sampler.

[6] To our knowledge, using distinct but related data to inform prior distributions, for example via power priors, is standard e.g. in the analysis of medicinal trials; see e.g. Ibrahim and Chen (2000) and Ibrahim et al. (2015).

3.3 Density forecasting and risk measurement

This section explains how forecasts can be generated from the recursive SQVAR model (9) without invoking parametric assumptions on the distribution of the endogenous variables. To focus on the main idea and simplify the exposition, we here consider a special case of (9), with $p = 1$ and $B(\gamma) = C_0(\gamma) = C_1(\gamma) = 0$.

Consider an n-vector $u_1^* \equiv [u_{11}^*, \ldots, u_{n1}^*]'$ whose elements are random draws from the i.i.d. uniform distribution with support on $(0, 1)$. Then a draw from the one-step ahead forecast distribution of x_{T+1} is:

$$x_{T+1}^* = (I_n - A_0(u_1^*))^{-1}(\omega(u_1^*) + A_1(u_1^*)x_T)$$

where I_n is the n-dimensional identity matrix, and we have replaced the vector of quantile probabilities γ with the random realization u_1^*. The quantile parameters associated with u_1^* can be estimated (or were already estimated previously and then stored).

Conditional on this draw, a draw from the two-step ahead forecast distribution of x_{T+2} is

$$x_{T+2}^* = (I_n - A_0(u_2^*))^{-1}(\omega(u_2^*) + A_1(u_2^*)x_{T+1}^*),$$

where u_2^* is another n-vector with i.i.d. random draws from the standard uniform distribution. Iterating this process forward, it is possible to obtain a sample path $(x_{T+1}^*, x_{T+2}^*, \ldots, x_{T+H}^*)$ of any desired length H. The SQVAR's recursive structure (9) and Lemma 1 of Wei (2008) ensure that there is a one-to-one continuous mapping between the sample space x_{T+t} and the hypercube $(0, 1)^n$ generated by the random draws u_t^*, for $t = 1, \ldots, p$; see Chavleishvili and Manganelli (2023) for a discussion.

With n variables, q quantiles, and H steps ahead, there are q^{nH} possible paths at any time $t = 1, \ldots, T$. To explore the "tree" of all potential future paths at any time, we randomly generate S future paths for all n variables in x_{t+h}, $h = 1, \ldots, H$ quarters ahead. Once predictive densities

are available, the estimation of downside risk measures is straightforward. At each $t + h$, we calculate the required measures of downside risk and upside potential; Web Appendix B provides the necessary details.

3.4 Quantile impulse response functions

We obtain quantile impulse response function estimates by simulation. Intuitively, given a draw from the parameters' posterior distribution, a structural shock to any variable can be propagated forward using (9). Doing this many times allows us to obtain predictive quantiles of all variables in the system at any horizon $h = 1, \ldots, H$. These predictive quantiles are compared to their no-shock counterparts, which are also obtained by simulation. Obtaining QIRF estimates in this way requires a loop within a loop: an outside loop drawing from the posterior density of the parameters, and an inside loop propagating forward both the shock and no-shock scenarios. Web Appendix B.1 provides the algorithm and discusses implementation details.

3.5 Counterfactual scenarios

Rather than moving through the tree of potential future values of x_{t+h} completely at random, as just explained, we can also focus on a subset of potential paths, or, in the extreme, consider only one path in isolation. Such a subset of potential paths can be thought of as a counterfactual 'scenario,' or model-based thought experiment, that conditions on an arbitrary but fixed sequence of future shocks for a strict subset of variables in x_t. We use such scenarios when considering a model-based stress test in Section 5.4, and when studying the benefits vs. cost from tightening macro-prudential policy stance in Section 5.5. Web Appendix B.3 provides additional detail.

4 Euro area data

4.1 GDP and inflation data pre-1999

Structural QVAR models require a sufficiently large sample size to ensure that their parameters can be estimated with adequate precision. The euro area, however, celebrated its 20th anniversary only in 2019. When working with quarterly data, $T = 4 \times 23 = 92$ is at the low end of what is required for a meaningful empirical study of macro-financial interactions at different quantiles, particularly when the SQVAR model contains multiple lags.

We address this challenge in two ways. First, we use non-diffuse priors to inform our empirical analysis; see Section 3.2. Second, we use pre-1999 macro-financial time series data for the euro area when available. Such pre-1999 data were urgently needed for monetary policy analysis during the ECB's early years. As a result, counterfactual data were constructed "as if" the euro area had already existed earlier. Pre-1999 euro area data is publicly available;[7] see e.g. Fagan et al. (2001). We obtain quarterly real GDP and monthly consumer price index data between 1990Q1 and 1998Q4 from this source and splice it with official Eurostat data on real GDP and the Harmonised Index of Consumer Prices (HICP) between 1999Q1 and 2022Q4. Quarterly consumer prices are then computed as averages of monthly index levels. This results in $T = 132$.

4.2 Composite indicator of systemic stress

As a measure of system-wide financial distress, we use the revised daily version of the ECB's composite indicator of systemic stress (CISS) as introduced and described in Chavleishvili and Kremer (2023). This version of the CISS includes 15 individual market-based financial stress indicators that cover the main segments of a typical modern financial system: financial intermediaries, money markets, equity markets, bond markets, and foreign exchange markets. The 15 indicators are aggregated into a single statistic in a way that takes their time-varying cross-correlations into account. As a result, the CISS takes higher values when stress prevails in most market segments

[7] https://eabcn.org/page/area-wide-model.

at the same time, capturing the idea that financial stress is more systemic, and more dangerous for the economy as a whole, whenever financial instability spreads widely across different parts of the financial system. The CISS for the euro area (as well as that for the U.S. and other countries) is updated daily and publicly available via the ECB's Statistical Data Warehouse.[8] Figure C.1 in Web Appendix C provides a time series plot of quarterly averages of daily CISS data.

4.3 The financial cycle

The financial cycle indicator used in the empirical analysis is based on Lang et al. (2019). It is designed to capture risks stemming from domestic (real) credit volumes, real estate markets, asset prices, and external imbalances. Lang et al. (2019) demonstrate that the indicator increases, on average, three to four years before the onset of systemic financial crises and the ensuing economic recession, and that its early warning properties for euro area countries are superior to those of the total credit-to-GDP gap, a popular alternative referred to in Basel-III regulation. As a result, the financial cycle measurement offers useful information about both the probability and the likely cost of systemic financial crises several years in advance. In our model, a systemic financial crisis entails a sharp increase in the CISS and a subsequent large drop in real GDP.

Figure C.1 in Web Appendix C provides a time series plot of the financial cycle indicator. It takes high values during the dot-com boom years between 1997 and 2000 and during the credit boom years preceding the 2008–2009 global financial crisis. The financial cycle takes particularly low values in 2009 and 2011, at times associated with crisis-induced fire sales and financial system deleveraging.

4.4 Short-term interest rates

To construct a consistent time series of short-term euro area interest rates, we splice together three time series, as follows. From 1999Q1 to 2022Q4, we use quarterly averages of the three-months-ahead euro Overnight Index Swap (OIS) rate, a risk-free interest rate. Between 1994Q1

[8] https://sdw.ecb.europa.eu/

and 1998Q4, we use the three-month Euro Interbank Offered Rate (EURIBOR), corrected for the average EURIBOR-OIS spread between 2000Q1 and 2007Q2. Finally, between 1990Q1 and 1993Q4, we use the German Frankfurt Interbank Offered Rate (FIBOR), additionally adjusted for the average FIBOR-EURIBOR spread between 1994Q1 and 1998Q4. All interest rate data are taken from London Stock Exchange Group. Web Appendix C provides a time series plot.

5 Implementing the risk management approach

This section first discusses model selection, parameter estimates, and quantile impulse response function estimates. It then discusses downside risks to the euro area economy and the outcome of a macro stress testing exercise. Finally, it offers a metric of the macro-prudential policy stance designed to help assess whether a tightening (leaning against the financial cycle) or a loosening of macro-prudential policy would yield beneficial outcomes.

5.1 Model specification

We select a $n = 5$-variable SQVAR model (9) with $p = 4$ lags as our preferred model.[9] Specifically, the vector of endogenous variables x_t contains a financial cycle indicator c_t, annualized quarter-on-quarter HICP inflation π_t, annualized quarter-on-quarter real GDP growth y_t, the CISS s_t, and the three-month OIS interest rate r_t, $x_t = (c_t, \pi_t, y_t, s_t, r_t)'$.[10] Slow-moving variables, such as the financial cycle (which is constructed from multi-year growth rates), inflation, and real GDP growth, are ordered first, while fast-moving financial variables, such as the CISS and the OIS rate, are ordered last. The ordering of variables identifies the contemporaneous correlations between the endogenous model variables according to the recursive information set defined in Section 3.1.

[9] Information criteria, such as the Deviance Information Criterion DIC, AIC, and BIC, point to different numbers of lags p, depending on the considered criterion, variable, and quantile. Weighing all evidence, $p = 4$ is at the conservative upper end of the indicated values.

[10] The ECB working paper version of this paper undertakes an extensive variable selection exercise, indicating that short-term interbank rates can be a useful variable to consider in an SQVAR. In addition, short-term interest rates have been linked to the accumulation of financial vulnerabilities over time, see e.g. Boissay et al. (2016), and to increasing leverage and reach-for-yield behavior in financial markets, see e.g. Brunnermeier and Sannikov (2014) and Akinci et al. (2020). Short-term interest rates, in turn, respond to GDP and inflation through systematic monetary policy.

We include a global commodity price index (Standard and Poor's GSCI index; formerly the Goldman Sachs Commodity Index) as an exogenous variable z_t in (9), and also consider $p = 4$ lags there. The parameters are restricted such that global commodity prices can only impact inflation directly; this prevents a positive response of GDP to a global negative supply shock. We also include four dummy variables d_t that correspond to four Covid-related observations between 2020Q1 and 2020Q4. This inclusion effectively neutralizes the effect of these Covid-related observations on the posterior parameter estimates.

Finally, we follow Estrella (2015) and impose a transmission-lag on the direct (structural) impact of short-term interest rates on the real economy. As a result, two elements of $A_1(\gamma)$, one in the inflation and one in the real GDP row, are restricted to zero. Short-term interest rates (monetary policy) can then still have a first-lag impact on the real economy, but only through the financial cycle (ordered first in x_t).

5.2 Parameter estimates and impulse response functions

Web Appendix D presents posterior mean estimates of the vector of intercepts ω, the triangular matrix A_0, and the lag matrices A_1 to A_4. Posterior mean estimates are shown with corresponding 95% equally-tailed credible intervals. Least squares parameter estimates are visible as horizontal lines and are provided as a point of comparison. The posterior parameter estimates are obtained equation-by-equation via nq univariate Bayesian quantile regressions; see Section 3.2. Web Appendix E presents the analogous estimates for U.S. data.

The parameter estimates differ substantially across quantiles, and also from their ordinary least-squares counterparts. E.g., the contemporaneous impact parameters in A_0 are often close to zero around the median, but are in some cases different from zero for tail quantiles. As one example, the contemporaneous impact of a shock to the financial cycle on financial stress (element [4,1] in A_0) is close to zero to the left of the median and negative for the upper quantiles. As a second example, the contemporaneous impact of a shock to financial stress on short-term interest rates (element [5,4] in A_0) is close to zero to the right of the median and negative for the lower quantiles.

Figure 1: Selected quantile impulse response functions

Quantile impulse response functions for the financial cycle, real GDP growth, and the CISS as implied by the posterior estimates reported in Web Appendix D. Credible bands are at a 95% confidence level, and based on 400 draws from the posterior distribution and 20,000 forward simulations for each draw. The shock size is chosen as one standard deviation of the residuals from the median quantile regression of the respective variables. The estimation sample is 1990Q1 to 2022Q4. Web Appendix D presents the full 5×5 set of QIRFs, and also presents the median response.

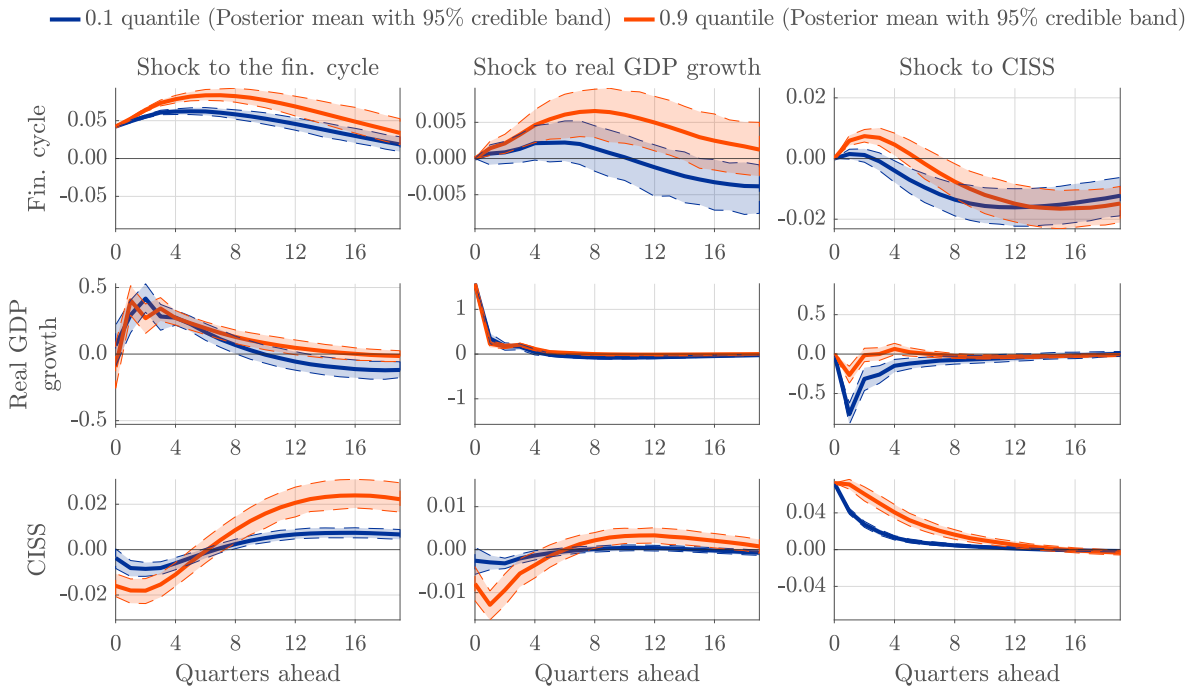

Parameter heterogeneity across quantiles is also present for the lagged parameter matrices A_1 to A_4. For example, the [3,4]-element of A_1 signals the presence of substantial asymmetries in the impact of financial stress (CISS) on future real GDP growth: the lower quantiles are much more affected.

Figure 1 plots a selection of quantile impulse response functions (QIRF) as implied by the parameter estimates for the upper (90th percentile) and lower tails (10th percentile) of variables relevant for the macro-prudential policymaker: the financial cycle, real GDP growth, and the CISS. The QIRFs summarise all the direct and indirect, contemporaneous and lagged relationships between the endogenous model variables. The generally rather low contemporaneous relationships between the model variables (captured via A_0; see Web Appendix D) imply that the QIRF are qualitatively but also quantitatively largely independent of the specific ordering of the variables in

x_t. To economize on space, the entire set of QIRFs for all endogenous variables and shocks, also including the median QIRF, can be found in Figure D.10 in Web Appendix D.

In some cases the QIRFs show pronounced asymmetries, while in other cases the differences between the quantiles are both small and within the credible intervals, representing more or less linear relationships between the model variables. Consistent with the vulnerable growth literature (e.g., Adrian et al., 2019, Adrian et al., 2021), the response of real GDP growth to a shock in the CISS (Figure 1's panel [2,3]) is much stronger in the left tail (the 0.1 quantile) of the growth distribution than in its center and right tail (the 0.9 quantile). Thus, a given increase in financial stress depresses economic growth much more strongly in the lower part of the distribution than in the upper part.

The response of the CISS to a shock to the financial cycle (Figure 1's panel [3,1]) indicates an initial dampening of stress followed by an increase after approximately two years. This pattern is particularly pronounced for the upper 0.9 quantile of the CISS, which displays a marked negative response in the short term that reverses after approximately six quarters and subsequently overshoots. Vice versa, positive shocks to the CISS depress the financial cycle in the medium term (Figure 1's panel [1,3]).

Taken together, the interactions between the CISS, real GDP growth, and the financial cycle point to the possibility of a vicious cycle during crisis periods, in which an increase in financial stress triggers a sharp reduction in economic activity, eventually leading to further financial stress. In addition, a reduction in financial stress today leads to more elevated systemic risk in the medium term. Such dynamics lend support to nonlinear macroeconomic models with a financial sector that feature occasionally binding (financing) constraints and a "financial stability-" or "volatility paradox," including Brunnermeier and Sannikov (2014), Boissay et al. (2016), He and Krishnamurthy (2019), and Mendicino et al. (2024).

Web Appendix E reports SQVAR parameter and credible interval estimates for U.S. data. The parameter estimates are broadly in line with those for the euro area. For example, growing financial vulnerabilities shift the right tail of the U.S. CISS towards more positive values. A shock to the

U.S. CISS shifts the left tail of the predictive GDP growth distribution towards more negative values while leaving the right tail less affected.

5.3 Estimates of downside risk and upside potential

This section discusses estimates of downside risk and upside potential as defined in Section 2.1. It considers both quantile- and expectation-based measures.

Figure 2 plots two estimates of GaR, the 5% and 10% predictive quantile of real GDP growth, at any time t. Three other quantiles (the median, 90%, and 95%) are reported to indicate upside potential and for comparison. All estimates are based on the same (full-sample) parameter estimates but are otherwise conditional on variables observed up to time t only. The predictive densities correspond to four different forecast horizons: one quarter ahead, one year ahead, one year ahead one year out, and one year ahead four years out.

We highlight two results. First, as a result of macro-financial interactions, the SQVAR's lower quantiles for future real GDP growth are considerably more volatile than its upper quantiles. For the one-quarter-ahead forecast, the predictive quantiles' standard deviations decrease almost monotonically as the quantiles increase: from 2.66 and 2.59 for the 5% and 10% quantile, to 1.85 for the median quantile, to 1.44 and 1.53 for the 90% and 95% quantile. This result mirrors that of Adrian et al. (2019) for U.S. data.

Second, the asymmetry in the predictive density decreases with the forecasting horizon. For the one-year-ahead forecast, the predictive quantiles' standard deviations continue to decrease as the quantiles increase: from 1.73 and 1.61 for the 5% and 10% quantile, to 1.27 for the median, to 1.04 and 1.02 for the 90% and 95% quantile. For the one-year-ahead forecast four years out, the predictive quantiles' standard deviations still decrease as the quantiles increase, although the pattern is now more muted: from 0.49 and 0.43 for the 5% and 10% quantile, to 0.31 for the median, to 0.28 and 0.29 for the 90% and 95% quantile. We conclude that the asymmetry in the predictive density is considerably reduced but still noticeable after five years.

Figure 3 plots the average growth shortfall $\text{AGS}^{\tau}_{t,t+1:t+H}$ and average growth longrise $\text{AGL}^{\tau}_{t,t+1:t+H}$

Figure 2: Predictive quantiles for euro area real GDP growth

Selected predictive quantiles over different forecast horizons at any time. The top left and top right panels refer to the annualized one-quarter and one-year ahead growth rate. The bottom left and bottom right panels refer to the one-year-ahead growth rate one year out, and the one-year-ahead growth rate four years out. The forecasts are obtained by simulation using $S = 100,000$ at each t. SQVAR parameters are fixed at their full sample posterior mean estimated for $q = 19$ quantiles ranging from 0.05 to 0.95.

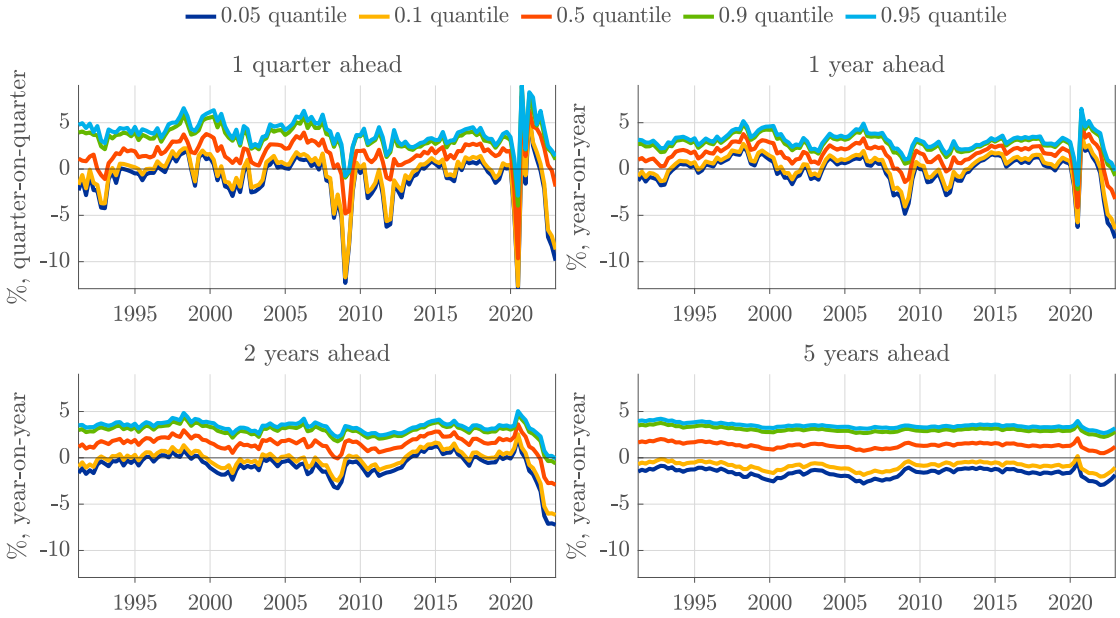

estimated at each point in time between 1990Q1 and 2022Q4, for $\tau = 0$, and $H = 4$ quarters (top panel) and $H = 8$ quarters ahead (bottom panel). To study the importance of including financial conditions and medium-term vulnerabilities in the econometric model, we here also compare our SQVAR model's estimates to those of a much simpler, univariate quantile autoregressive (QAR) model for GDP growth only. As a result, the QAR model includes only its own lags but not the financial cycle, the CISS, or any other variable.

We again highlight two results. First, accounting for financial conditions is important. There is a pronounced difference between the downside risk (AGS) estimate implied by the SQVAR and the univariate QAR. During the GFC in 2008 and 2009, the QAR-based downside risk estimate declines much later, and by much less, compared to the SQVAR-based estimate. In the context of the euro area sovereign debt crisis of 2010–2012, only the SQVAR indicates elevated downward risks to growth ahead of the recession of 2011–2012; by construction, the QAR model only

responds when the economy actually starts to contract. Similarly, towards the end of the sample, increased downside risks reflecting the bout in energy and consumer price inflation in 2021–2022, elevated financial stress, and rapid monetary policy tightening, only show up in the SQVAR. During the Covid-19 pandemic, both the SQVAR and QAR deliver similar upward and downward risks to growth. This is intuitive, as financial factors did not play a major role in bringing about the unprecedented stress.

Second, from a risk management perspective, the AGS can be compared to the AGL. The GFC, for example, did not only generate an extremely low value for the AGS but also for the AGL. With a value of only 0.8% (taken from Figure 3's bottom panel), the average expected expansion of the economy over the following two years would have been approximately 1.6%. This compares to an average of approximately 4% over the entire sample. The GFC thus reduced living standards especially because of the contraction, but also persistently muted the upside potential of the economy, and did so until early 2015.

5.4 Model-based macro stress testing

Macro-prudential policymakers suspect that the economy is not at all times equally robust to the materialization of financial shocks (Adrian et al. (2019). If so, policymakers need help deciding whether today, say, is a good time to tighten macro-prudential policy or not. This section discusses the outcome of a model-based stress testing exercise that can inform this question.

We here understand macro stress testing as a density forecast of what would happen to real GDP growth if the system is subjected to a certain sequence of adverse shocks. We refer to such a sequence as a stress scenario; see Section 3.5. Our stress testing approach is different from supervisory stress tests in that our main variables of interest are not banking sector variables but measures of macro-financial stability, particularly real GDP growth.

Figure 4 reports the time-t conditional forecast of average future real GDP growth $\bar{y}_{t+1:t+4}$ between time t and $t+4$ as implied by our model. The forecast is conditional on a 0.1 quantile realization of the financial cycle c_{t+h}, and a 0.9 quantile realization for the CISS s_{t+h}, consecu-

Figure 3: Euro area growth shortfall and longrise

Estimates of time-t average growth shortfall $\text{AGS}^{\tau}_{t,t+1:t+H}$ and average growth longrise $\text{AGL}^{\tau}_{t,t+1:t+H}$ evaluated at $\tau = 0$ and $H = \{4, 8\}$; see (3) and (5). Based on 200 draws from the posterior distribution and 50,000 forward simulations of the conditional distribution for each draw. The model is estimated for $q = 19$ quantiles ranging from 0.05 to 0.95. Quarterly annualized real GDP growth is reported for comparison (dotted black line, scale on right axis). Shaded areas indicate euro area recessions as determined by the CEPR business cycle dating committee. Credible intervals are dashed and at a 95% level.

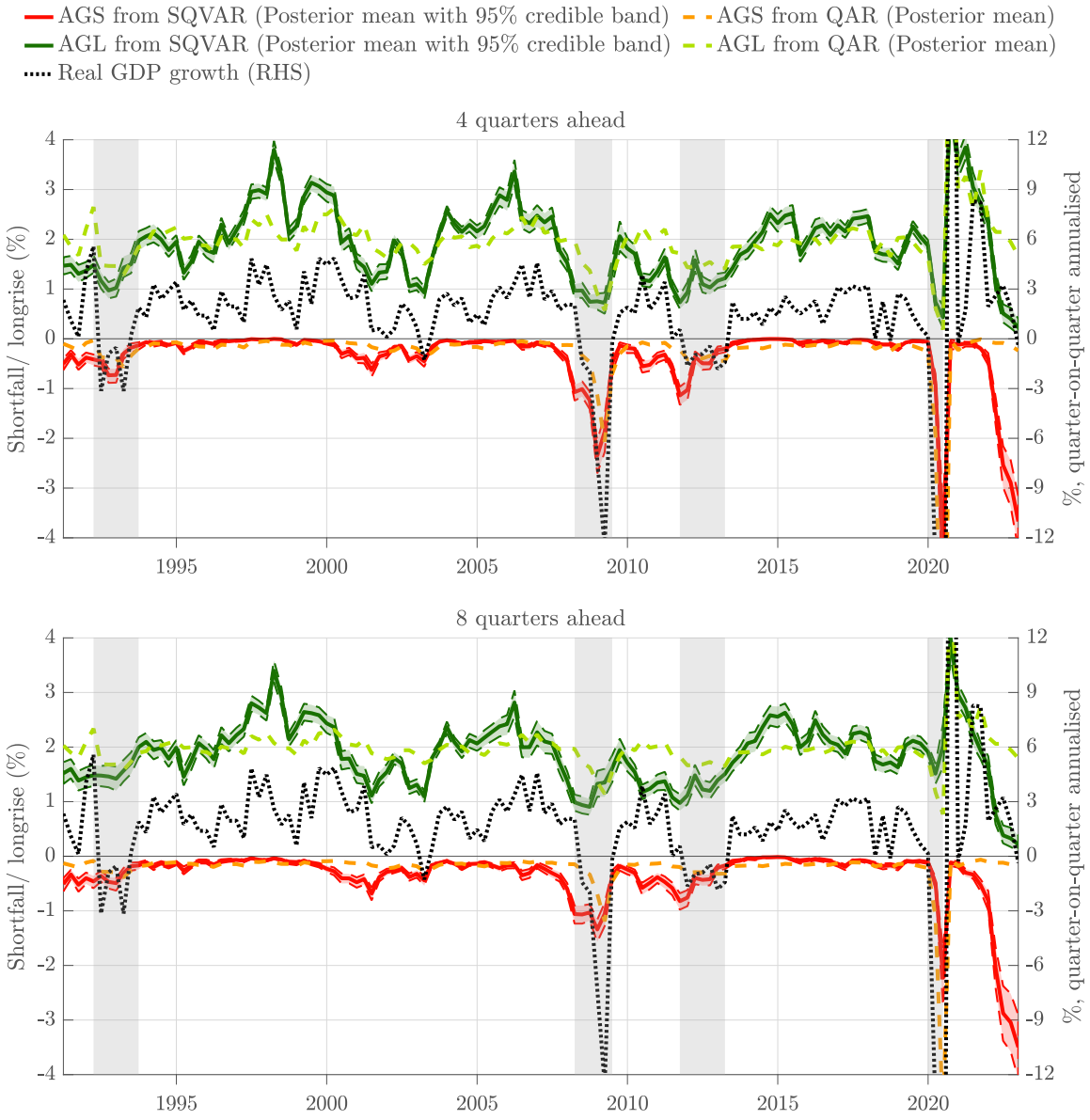

tively for $h = 1, \ldots, 4$. The magnitude of these shocks is comparable to the four observed quantile realizations for these variables between 2008Q1 and 2008Q4 during the GFC. The stress test (i.e.,

Figure 4: Vulnerability to GFC-sized shocks

Solid line: period-t predicted average annualized quarterly real GDP growth four quarters ahead, $\hat{\hat{y}}_{t+1:t+4}$ conditional on four consecutive 0.1 quantile realizations of the financial cycle c_t, and 0.9 quantile realizations for CISS s_t. The remaining variables' paths are unrestricted. Dotted line: realized annual average between $t+1$ and $t+4$, for comparison. Based on 1,000 draws from the full sample posterior distributions and one forward simulation per draw. Credible intervals are reported at a 95% level. Grey-shaded areas indicate CEPR-dated euro area recessions. The estimation sample is 1990Q1 – 2022Q4.

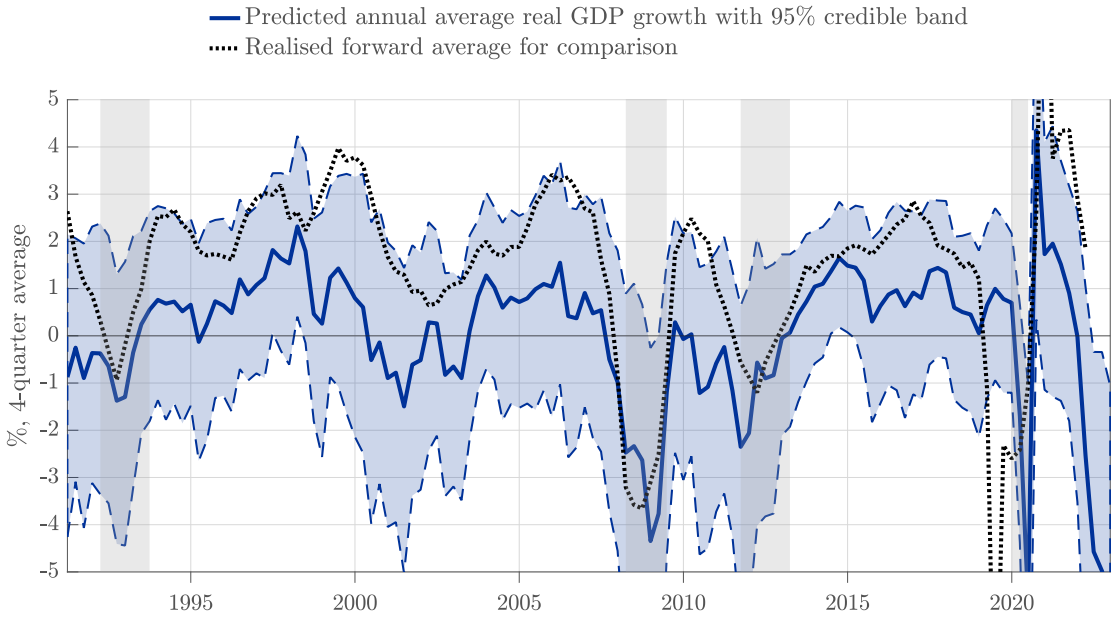

the same sequence of adverse shocks) is repeated at each $t = 1, \ldots, T$, and is always based on the same (full sample, posterior mean) parameter estimates. As a result, the figure is informative about the impact of GFC-sized financial shocks on economic activity at any time in our sample.[11]

Figure 4 suggests that the euro area economy is not equally resilient to the same sequence of equally unlikely adverse financial shocks at all times. This is a direct consequence of the asymmetries (nonlinearities) inherent in the estimated model. A comparison with Figure C.1 in Web Appendix C indicates that real GDP growth is particularly vulnerable after the financial cycle has taken high values, such as in years 1992, 2003, and 2008.

[11] Alternatively, one could define stress in absolute size; see e.g. Brownlees and Engle (2017) for a discussion. We prefer the quantile-based approach because the probability of the stress materializing remains constant over time regardless of current levels of volatility. In periods of low volatility, an absolute stress value would imply a much more severe and much less probable stress event, as it would take a sequence of more severe shocks, that is quantile realisations, to reach the necessary level of impact. On the other hand, low volatility does not necessarily imply that the tipping point is also low.

Figure 4 can also be informative when assessing the macro-prudential policy stance. An unusually high level of vulnerability to future real and financial shocks — a value of $\bar{y}_{t+1:t+4}$ below its unconditional 5% quantile, say — indicates that large shocks have materialized and macro-prudential buffers could be decreased. In the euro area, such values are observed during the financial crisis of 2008 – 2009 and the sovereign debt crisis in 2011 – 2012. Low to moderate levels of vulnerability indicate times when macro-prudential buffers could be built up, such as in the years around 2005 and 2015. Gradually growing macro-prudential buffers can help increase banking sector resilience, lean against unrestrained credit growth, improve risk-taking incentives (Admati and Hellwig, 2013), and are available to be decreased later if necessary.

5.5 Macro-prudential policy stance

An active debate in policy circles revolves around the question of how to measure the macro-prudential policy stance. In other words, should macro-prudential policy be tightened or loosened today conditional on currently available information? We use the decision framework in Section 2.3 to address this question.

We assume that macro-prudential instruments, including a counter-cyclical capital buffer, can be used to influence the financial cycle, and ask when it is beneficial to do so.[12] The thought experiment of this section is the following: How does the macro-prudential authority's objective function value (7) change if the financial cycle is marginally lowered now, to be increased later on? If the change is positive, we conclude that the macro-prudential stance is too loose (as it would benefit from a lower, less buoyant financial cycle). If, on the other hand, the answer is negative, then macro-prudential policy is too tight.

Table 1 summarizes our policy experiment by contrasting two counterfactual scenarios. Its top and bottom panels set out a passive macro-prudential policy scenario and an active macro-prudential policy scenario, respectively. Each scenario looks five years (20 quarters) into the future.

[12] A complete answer to this question would require including the macro-prudential policy instruments into our model. This could be done, in principle, if high-quality and up-to-date data on the timing and nature of macro-prudential policy actions were available, and at the cost of decreased model parsimony, parameter estimation precision, and, potentially, identification credibility. We leave this to future research.

In each case, the first six quarters are buoyant times during which the financial cycle could, in principle, be marginally reduced. Following a turn of the financial cycle (quarters 7 – 8), a short but severe financial crisis ensues (quarters 9 – 11), potentially impacting the macro-economy for a long time in its aftermath (quarters 12 – 20).

The active scenario is identical to the passive scenario, except that the policymaker decides to lean against the buoyant financial cycle during the first six quarters. For example, the policymaker could compel banks to comply with higher counter-cyclical capital buffer requirements during these times. During the financial crisis (in quarters 9–10), these buffers can then be decreased, leading to a marginally less vicious collapse of the financial cycle. We simulate this policy by setting the financial cycle to its 0.5 quantile during $h = 1, \ldots, 6$, instead of 0.7, and to its 0.4 conditional quantile during $h = 7, \ldots, 10$, instead of 0.2. The CISS takes high values, and the financial cycle takes low values, during the financial crisis in either scenario. The evolution of all other variables in the SQVAR (real GDP growth, inflation, and short-term interest rates) is unrestricted. Doing so allows us to simulate forward the GDP growth rate, y_{t+h}, and associated growth shortfalls, $\text{GS}_{t,t+h}$, at any time $t + h$, $h = 1, \ldots, 20$.

Each policy scenario is evaluated as

$$u_t\left(\text{Scenario}\right) = \hat{\bar{y}}_{t+1:t+20}\left(\text{Scenario}\right) + \left(\lambda^p - 1\right) \cdot \widehat{\text{AGS}}_{t,t+1:t+20}\left(\text{Scenario}\right), \tag{10}$$

where the mean growth estimate $\hat{\bar{y}}_{t+1:t+20}$ and average future growth shortfall estimate $\widehat{\text{AGS}}_{t,t+1:t+20}$ are obtained from 50,000 simulations of potential future values of y_{t+h}. We repeat this exercise 200 times, each time using a new draw from the parameters' posterior density. The objective function (10) operationalizes (7) by choosing parameters as $\delta = 1$ for $h = 1, \ldots, 20$ and $\delta = 0$ thereafter, $\lambda \in \{1.5, 3\}$, and $\tau = 0$. Our choice of the penalty term $\lambda^p = 1.5$ implies that the policymaker cares twice as much about future average growth than she cares about reducing downside risk. If $\lambda^p = 3$, then the policymaker is more risk averse and cares twice as much about reducing downside risk than she cares about fostering future average growth. We evaluate (10) twice, once for the

Table 1: Passive vs. active macro-prudential policy

Notes: The top and bottom panels report selected quantiles for the financial cycle (c_t) and CISS (s_t) under a passive and active macro-prudential policy benchmark, respectively. "–" implies that the quantile is picked at random. This is always the case for real GDP growth y_t, inflation π_t, and short-term interest rates r_t. The first six quarters are "sanguine times," during which the financial cycle could be marginally reduced. In quarters 7 and 8 the financial cycle begins to turn, taking low values. Quarters 9–11 constitute a financial crisis, during which the CISS takes high values and the financial cycle takes low values. Quarters 12–20 track the financial crisis' fallout. The quantile choices for the financial cycle in the top vs. bottom panel (0.7 vs. 0.5, and 0.2 vs. 0.4) reflect that the financial cycle does not have to contract as much during the crisis when it is managed during the first six quarters; see also the discussion in the main text.

		"sanguine times"	"turn of cycle"	"financial crisis"		"fallout"
$t+h$		1–6	7–8	9–10	11	12–20
Passive benchmark	y_t, π_t, r_t	–	–	–	–	–
	c_t	0.7	0.2	0.2	–	–
	s_t	–	–	0.9	0.9	–
Active policy	y_t, π_t, r_t	–	–	–	–	–
	c_t	0.5	0.4	0.4	–	–
	s_t	–	–	0.9	0.9	–

active scenario and once for the passive scenario, and study the difference between the two values at any time t.

Figure 5 presents the objective function difference $\Delta u_t = u_t\,(\text{active}) - u_t\,(\text{passive})$ associated with adopting the active macro-prudential policy along with 50% and 68% credible intervals. Adopting the active policy is the preferred option most of the time. This is not surprising, as we condition on a financial crisis later on. Adopting the active policy, however, is not equally beneficial at all times. The benefits from leaning against the financial cycle are maximal during the late 1990s before the bust of the dot-com boom in 2000, and during the mid-2000s before the onset of the global financial crisis in 2007. This is intuitive, as the financial system was buoyant during these times, arguably seeding the respective busts later on (Boissay et al., 2016).

The benefits from leaning against the financial cycle are estimated to be negative following the end of the dot-com boom in 2000, and during the GFC. This is again intuitive, as the financial system was already deleveraging during these times, and requiring more would add insult to in-

Figure 5: The benefits from active macro-prudential policy

The benefit of adopting an active macro-prudential policy stance in utility terms, $\Delta u_t = u_t\,(\text{active}) - u_t\,(\text{passive})$; see (10). Based on 200 draws from the posterior distribution and 50,000 forward simulations of the conditional distribution for each draw. Parameters are chosen as $\delta = 1$, $\tau = 0$, $H = 20$, and $\lambda^p \in \{1.5, 3\}$. The difference is based on full sample estimates. Credible intervals are dashed and at a 50% and 68% level, respectively. The estimation sample is 1990Q1 to 2022Q4. Shaded areas indicate CEPR-dated euro area recessions.

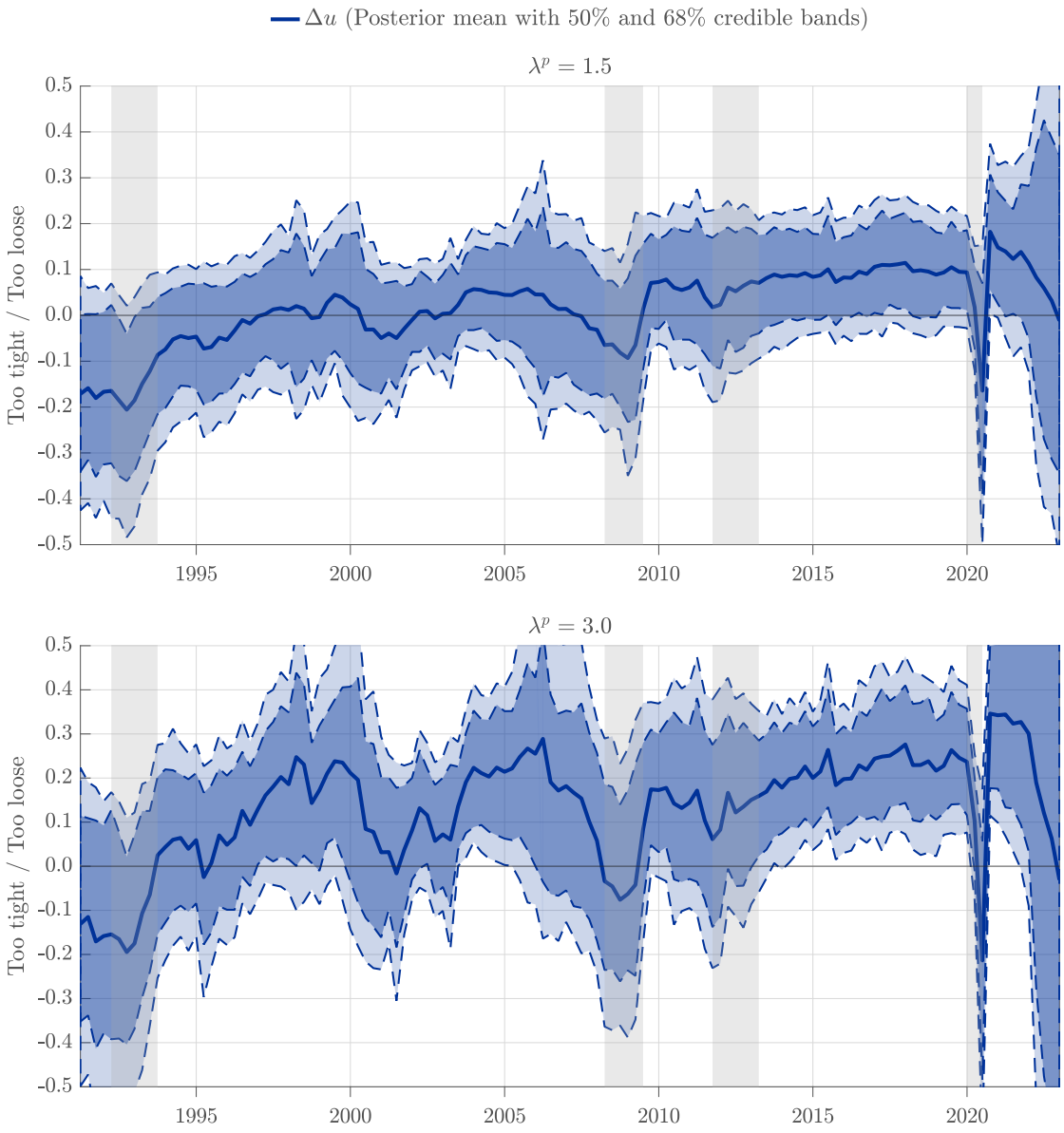

jury. The objective function difference Δu_t is mildly correlated with the euro area financial cycle, suggesting that it is a valuable variable to track to inform macro-prudential policy discussions.

Finally, we note that Δu_t in Figure 5 is estimated with considerable uncertainty. The zero

line is often inside the plotted credible intervals, suggesting that setting macro-prudential policy in practice is as much an art as it is (currently) a science.

Despite the surrounding uncertainty, Figure 5 may nevertheless suggest a potential rule-of-thumb to set the Basel-III counter-cyclical capital buffer in practice: increase the buffer by 0.25 percentage points every year, within the given regulatory range between zero and 2.5%, except when it's obvious that the economy is in, or about to enter, a contraction. In this way, the buffer can be brought from zero to full 2.5% capacity in ten years of expansion, in time to be ready for release during the next vicious financial crisis.

6 Conclusion

We formalized the macro-prudential authority's decision problem under uncertainty and studied it for the euro area. Flexible and potentially asymmetric predictive distributions are obtained from a semi-parametric structural quantile vector autoregressive model. This model allows us to study the nonlinear relationship between economic growth and various other factors such as financial stress, the financial cycle, short-term interest rates, and inflation. We documented substantial asymmetries in the predictive distribution of real GDP growth and the responses of macroeconomic variables to financial shocks. Considering counterfactual scenarios allowed us to perform a model-based stress testing exercise, assess macro-prudential policy stance, and study the conditions when macro-prudential interventions are most likely to be beneficial.

The paper presents several possible routes for future research. First, to our knowledge, shock identification for Quantile VAR models, e.g. through sign restrictions or external instruments, is currently a wide-open field (Chavleishvili and Manganelli, 2023, Iacopini et al., 2024). Second, panel-SQVAR approaches could be considered theoretically and empirically, possibly incorporating hierarchical specifications of random coefficients as in, e.g., Jarocinski (2010). Finally, the relative out-of-sample density forecasting performance of various recent macro-at-risk models, and combinations thereof, is of substantial interest but has, to our knowledge, not yet been studied.

References

Admati, A. and M. Hellwig (2013). *The banker's new clothes: What's wrong with banking and what to do about it*. Princeton: Princeton University Press.

Adrian, T., N. Boyarchenko, and D. Giannone (2019). Vulnerable growth. *American Economic Review 109*(4), 1263–89.

Adrian, T., N. Boyarchenko, and D. Giannone (2021). Multimodality in macro-financial dynamics. *International Economic Review 62*(2), 861–86.

Adrian, T., F. Grinberg, N. Liang, and S. Malik (2022). The term structure of growth-at-risk. *American Economic Journal: Macroeconomics 14*(3), 283–323.

Akinci, O., G. Benigno, M. Del Negro, and Q. Albert (2020). The financial (in)stability real interest rate, r**. *Federal Reserve Bank of New York Staff Reports 946*.

Almon, S. (1965). The distributed lag between capital appropriations and net expenditures. *Econometrica 33*, 178–196.

Artzner, P., F. Delbaen, J. M. Eber, and D. Heath (1999). Coherent measures of risk. *Mathematical Finance 9*(3), 203–228.

Boissay, F., F. Collard, and F. Smets (2016). Booms and banking crises. *Journal of Political Economy 124*(2), 489–538.

Brandao-Marques, L., G. Gelos, M. Narita, and E. Nier (2020). Leaning against the wind: An empirical cost-benefit analysis. *IMF Working Paper*, 1–54.

Brownlees, C. and R. F. Engle (2017). SRISK: A Conditional Capital Shortfall Measure of Systemic Risk. *The Review of Financial Studies 30*(1), 48–79.

Brownlees, C. and A. B. M. Souza (2020). Backtesting global growth-at-risk. *Journal of Monetary Economics, forthcoming*.

Brunnermeier, M., A. Crocket, C. Goodhart, A. Persaud, and H. Shin (2009). The fundamental principles of financial regulation. *Geneva Report on the World Economy 11*.

Brunnermeier, M. K. and Y. Sannikov (2014). A macroeconomic model with a financial sector. *The American Economic Review 104*(2), 379–421.

Caldara, D., C. Scotti, and M. Zhong (2021). Macroeconomic and financial risks: A tale of volatility. *Federal Reserve Board International Finance discussion papers*.

Carlier, G., V. Chernozhukov, and A. Galichon (2016). Vector quantile regression: An optimal transport approach. *The Annals of Statistics 44(3)*, 1165 – 1192.

Carney, M. (2020). The grand unifying theory (and practice) of macroprudential policy. *Speech given at University College London on 5 March 2020*, 1 – 22.

Carriero, A., T. E. Clark, and M. Marcellino (2023). Capturing macroeconomic tail risks with Bayesian vector autoregressions. *Journal of Money, Credit and Banking, forthcoming 2023*.

Cecchetti, S. G. (2006). Measuring the macroeconomic risks posed by asset price booms. *NBER Working Paper No. 12542*, 1–31.

Cecchetti, S. G. and H. Li (2008). Measuring the impact of asset price booms using Quantile Vector Autoregressions. *unpublished manuscript*, 1–31.

Chavleishvili, S. and M. Kremer (2023). Measuring systemic financial stress and its risks for growth. *ECB Working Paper 2842*, 1 – 43.

Chavleishvili, S. and S. Manganelli (2023). Forecasting and stress testing with quantile vector autoregression. *Journal of Applied Econometrics, forthcoming*.

Chernozhukov, V. and I. Fernandez-Val (2011). Inference for extremal conditional quantile models, with an application to market and birthweight risks. *The Review of Economic Studies 112*, 1 – 41.

de Larosiere, J. (2009). The high level group on financial supervision in the E.U. *Report for the European Commission*.

De Santis, R. and W. van der Veken (2020). Forecasting Macroeconomic Risk in Real Time: Great and Covid-19 Recessions. *ECB Working Paper forthcoming*.

Delle Monache, D., A. De Polis, and I. Petrella (2023). Modeling and forecasting macroeconomic downside risk. *Journal of Business and Economic Statistics, forthcoming*.

Duprey, T. and A. Ueberfeldt (2020). Managing GDP tail risk. *Bank of Canada working paper 2020–03*, 1–63.

ECB (2019). European Central Bank Financial Stability Review, May 2019. .

Estrella, A. (2015). The price puzzle and VAR identification. *Macroeconomic Dynamics 19*(8), 1880–1887.

Fagan, G., J. Henry, and R. Mestre (2001). An area-wide model (AWM) for the euro area. *ECB Working Paper 42*.

Forni, M., L. Gambetti, and L. Sala (2021). Downside and Upside Uncertainty Shocks. *mimeo*, 1–63.

FSB (2009). Report to G20 Finance ministers and governors: Guidance to assess the systemic importance of financial institutions, markets and instruments – initial considerations. *www.fsb.org*.

Giannone, D., M. Lenza, and G. E. Primiceri (2015). Prior selection for vector autoregression. *The Review of Economics and Statistics 97*(2), 436–451.

Greenspan, A. (2003). Opening Remarks to Monetary policy and uncertainty: Adapting to a changing economy. In *Proceedings of the Federal Reserve Bank of Kansas City Symposium*, pp. 1–12. Carnegie-Rochester conference series on public policy.

He, Z. and A. Krishnamurthy (2019). A macroeconomic framework for quantifying systemic risk. *American Economic Journal: Macroeconomics 11*(4), 1–37.

Iacopini, M., A. Poon, L. Rossini, and D. Zhu (2023). Bayesian mixed-frequency quantile vector autoregression: Eliciting tail risks of monthly US GDP. *Journal of Economic Dynamics and Control 157*(104757), 1–22.

Iacopini, M., F. Ravazzolo, and L. Rossini (2024). Bayesian multivariate quantile regression with alternative time-varying volatility specifications. *mimeo*.

Ibrahim, J. G. and M.-H. Chen (2000). Power prior distributions for regression models. *Statistical Science 15*(1), 46–60.

Ibrahim, J. G., M.-H. Chen, Y. Gwon, and F. Chen (2015). The power prior: Theory and applications. *Statistics in Medicine 34*(28), 3724–3749.

IMF (2017). Global financial stability report: Is growth at risk? *IMF Global Financial Stability Report 3*, 91–118.

Iseringhausen, M., I. Petrella, and K. Theodoridis (2024). Aggregate skewness and the business cycle. *Review of Economics and Statistics, forthcoming*.

Jarocinski, M. (2010). Responses to monetary policy shocks in the east and the west of Europe: a comparison. *Journal of Applied Econometrics 25*(5), 833–868.

Khare, K. and J. P. Hobert (2012). Geometric ergodicity of the Gibbs sampler for Bayesian quantile regression. *Journal of Multivariate Analysis 112*, 108–116.

Kilian, L. and S. Manganelli (2008). The central banker as a risk manager: Estimating the Federal Reserve's preferences under Greenspan. *Journal of Money, Credit, and Banking 40*, 1103–1129.

Koenker, R. and Z. Xiao (2006). Quantile autoregression. *Journal of the American Statistical Association 101*(475), 980–990.

Korobilis, D. and M. Schröder (2023). Monitoring multicountry macroeconomic risk. *University of Glasgow mimeo*.

Koyck, L. M. (1954). *Distributed lags and investment analysis*. North-Holland, Amsterdam.

Kozumi, H. and G. Kobayashi (2011). Gibbs sampling methods for Bayesian quantile regression. *Journal of Statistical Computation and Simulation 81*(11), 1565–1578.

Lang, J. H., C. Izzo, S. Fahr, and J. Ruzicka (2019). Anticipating the bust: a new cyclical systemic risk indicator to assess the likelihood and severity of financial crises. *ECB Occasional Paper No. 219*, 1 – 77.

McNeil, A., R. Frey, and P. Embrechts (2005). *Quantitative Risk Management*. Princeton: Princeton University Press.

Mendicino, C., K. Nikolov, J. Rubio-Ramirez, J. Suarez, and D. Supera (2024). Twin defaults and capital requirements. *Journal of Finance, forthcoming*.

New York Fed (2022). Outlook-at-Risk: real GDP Growth, unemployment, and inflation. *https://www.newyorkfed.org/research/policy/outlook-at-risk.*.

Plagborg-Moller, M., L. Reichlin, G. Ricco, and T. Hasenzagl (2020). When is growth at risk? *Brookings Papers on Economic Activity*.

Prasad, A., S. Elekdag, P. Jeasakul, R. Lafarguette, A. Alter, A. F. Xiaochen, and C. Wang (2019). Growth at risk: Concept and applications in IMF country surveillance. *IMF Working Paper*.

Sims, C. A. (1980). Macroeconomics and reality. *Econometrica 48*, 1–48.

Suarez, J. (2021). Growth-at-risk and macroprudential policy design. *CEMFI mimeo*.

Van der Ghote, A. (2021). Interactions and coordination between monetary and macro-prudential policies. *American Economic Journal: Macroeconomics 13*(1), 1–34.

Wei, Y. (2008). An approach to multivariate covariate-dependent quantile contours with application to bivariate conditional growth charts. *Journal of the American Statistical Association 103(481)*, 397 – 409.

White, H., T. H. Kim, and S. Manganelli (2015). VAR for VaR: Measuring tail dependence using multivariate regression quantiles. *Journal of Econometrics 187*, 169–188.

Yu, K. and R. A. Moyeed (2001). Bayesian quantile regression. *Statistics & Probability Letters 54*, 437–447.

Web Appendix to

The risk management approach

to macro-prudential policy*

Sulkhan Chavleishvili,[(a)] *Robert F. Engle,*[(b)] *Stephan Fahr,*[(c)]

Manfred Kremer,[(c)] *Frederik Lund-Thomsen,*[(c)] *Simone Manganelli,*[(c)]

Bernd Schwaab[(c)]

[(a)] Aarhus University, [(b)] NYU Stern School of Business, [(c)] European Central Bank

*E-mail contacts: sulkhan.chavleishvili@econ.au.dk; rengle@stern.nyu.edu; stephan.fahr@ecb.europa.eu; manfred.kremer@ecb.europa.eu; frederik_ole.lund-thomsen@ecb.europa.eu; simone.manganelli@ecb.europa.eu; bernd.schwaab@ecb.europa.eu (corresponding author). The views expressed in this paper are those of the authors and they do not necessarily reflect the views or policies of the European Central Bank.

A Bayesian estimation

A.1 Gibbs sampler

We obtain posterior inference relying predominantly on established methods for Bayesian quantile regressions (see e.g. Yu and Moyeed, 2001, Kozumi and Kobayashi, 2011, Khare and Hobert, 2012, and Korobilis, 2017). This still allows us, as in Chavleishvili and Manganelli (2023), to estimate the SQVAR equation by equation. We start by considering the endogenous variable x_i at quantile γ,

$$x_{it} = w_{it}'\beta_i(\gamma) + \varepsilon_{it}^{\gamma}, \tag{A.1}$$

where x_{it} is a scalar, $i = 1, \ldots, n$, $t = 1, \ldots, T$, w_{it} is a vector of regressors (in our case, contemporaneous values and lags of the endogenous and exogenous variables, a constant, as well as dummy variables), and $\beta_i(\gamma)$ is a vector of quantile-specific coefficients. The error term $\varepsilon_{it}^{\gamma}$ is assumed to have an asymmetric Laplace distribution of the form

$$f\left(\varepsilon_{it}^{\gamma}\right) = \gamma\left(1-\gamma\right)\left[\sigma_i(\gamma)\right]^{-1} e^{-\rho_\gamma\left(\varepsilon_{it}^{\gamma}\right)}, \tag{A.2}$$

where $\sigma_i(\gamma)$ is a scale parameter, and $\rho_\gamma\left(\varepsilon\right) \equiv \varepsilon(\gamma - I(\varepsilon < 0))$ is the standard quantile regression check function; see also Koenker and Bassett Jr (1978) and Engle and Manganelli (2004). It is clear from (A.2) that minimizing the usual quantile regression objective function, as e.g. defined in Koenker and Bassett Jr (1978), is equivalent to maximizing a corresponding asymmetric Laplace log-likelihood; see e.g. Yu and Moyeed (2001).

An asymmetric Laplace random variable can be represented as a mixture of a standard normal and an exponential random variable (Yu and Moyeed, 2001, Kozumi and Kobayashi, 2011). As a result, (A.1) can be restated as

$$x_{it} = w_{it}'\beta_i(\gamma) + \theta(\gamma)\nu_{it}(\gamma) + \tilde{\tau}(\gamma)\sqrt{\sigma_i(\gamma)\nu_{it}(\gamma)}u_{it}^{\gamma}, \tag{A.3}$$

where $\tilde{\tau}^2(\gamma) = \frac{2}{\gamma(1-\gamma)}$, $\theta(\gamma) = \frac{1-2\gamma}{\gamma(1-\gamma)}$, $u_{it}^{\gamma} \sim N(0,1)$, $\nu_{it}(\gamma) \sim \mathcal{E}(\sigma_i(\gamma))$, and where $\mathcal{E}(\tilde{e})$ denotes an exponential distribution with mean $\tilde{e}$.

Since this section exclusively considers univariate regressions at a single quantile γ, we drop the quantile notation for convenience and leave the dependence implied. The mixture representation in (A.3) allows us to draw from the conditional posterior distributions using an appropriate set of prior distributions. We follow Kozumi and Kobayashi (2011) and choose the prior distributions

$$\beta_i \sim N\left(\underline{\mu}_{\beta,i}, \lambda_i \underline{\Sigma}_{\beta,i}\right), \qquad \sigma_i \sim IG\left(\underline{\alpha}_{\sigma,i}, \underline{\zeta}_{\sigma,i}\right), \tag{A.4}$$

where $IG(\alpha, \zeta)$ denotes an inverse-gamma distribution with shape and scale parameters α and ζ. The addition of the scalar $\lambda_i \geq 0$ to the prior variance of β_i lets us control the looseness/tightness of the respective prior. A lower value of λ_i implies a tight, informative prior, while a high value of λ_i implies a loose, uninformative prior. We give λ_i its own prior density and let $\lambda_i \sim IG(\underline{\alpha}_{\lambda}, \underline{\zeta}_{\lambda})$.

With the above priors in place, and continuing to rely on Kozumi and Kobayashi (2011) and Khare and Hobert (2012), we end up with the following four-step Gibbs sampler for all nq equations, dropping subscript i for convenience. Steps 1 – 3 are identical to those in Khare and Hobert (2012). Step is 4 is new but straightforward; Section A.3 provides a derivation.

1. Draw $\sigma|x, w, \ldots \sim IG\left(\bar{\alpha}_{\sigma}, \bar{\zeta}_{\sigma}\right)$,
   where $\bar{\alpha}_{\sigma} = \underline{\alpha}_{\sigma} + \frac{3}{2}T$, and $\bar{\zeta}_{\sigma} = \zeta_{\sigma} + \sum_{t=1}^{T} \frac{(x_t - w_t'\beta - \theta\nu_t)^2}{2\tilde{\tau}^2\nu_t} + \sum_{t=1}^{T} \nu_t$.

2. Draw $\beta|x, w, \ldots \sim N\left(\bar{\mu}_{\beta}, \bar{\Sigma}_{\beta}\right)$,
   where $\bar{\Sigma}_{\beta}^{-1} = \sum^{T} \frac{w_t w_t'}{\tilde{\tau}^2\sigma\nu_t} + \lambda^{-1}\underline{\Sigma}_{\beta}^{-1}$, and $\bar{\mu}_{\beta} = \bar{\Sigma}_{\beta}\left[\sum^{T} \frac{w_t(x_t - \theta\nu_t)}{\tilde{\tau}^2\sigma\nu_t} + \lambda^{-1}\underline{\Sigma}_{\beta}^{-1}\underline{\mu}_{\beta}\right]$.

3. Draw $\nu_t^{-1}|x_t, w_t, \ldots \sim \mathcal{IGN}(\bar{\kappa}_1, \bar{\kappa}_2)$, where $\mathcal{IGN}$ denotes the inverse Gaussian distribution, with $\bar{\kappa}_1 = \frac{\sqrt{\theta^2 + 2\tilde{\tau}^2}}{|x_t - w_t'\beta|}$, and $\bar{\kappa}_2 = \frac{\theta^2 + 2\tilde{\tau}^2}{\sigma\tilde{\tau}^2}$.

4. Draw $\lambda|\beta, \ldots \sim IG\left(\bar{\alpha}_{\lambda}, \bar{\zeta}_{\lambda}\right)$,
   where $\bar{\alpha}_{\lambda} = \underline{\alpha}_{\lambda} + \frac{\tilde{k}}{2}$, $\bar{\zeta}_{\lambda} = \zeta_{\lambda} + \frac{1}{2}\left(\beta - \underline{\mu}_{\beta}\right)' \underline{\Sigma}_{\beta}^{-1}\left(\beta - \underline{\mu}_{\beta}\right)$, and $\tilde{k}$ is the dimension of β (the number of regressors).

To conclude, we note that the Gibbs sampler of Kozumi and Kobayashi (2011) and Khare and Hobert (2012), steps 1–3 above, comes with theoretical guarantees: draws from the sampler converge to the intractable true posterior, and do so at a geometric rate. To prove this result, Khare and Hobert (2012) make no assumptions regarding the dimensions of the data (so that the result continues to hold even if $\tilde{k}$ were large relative to T).

A.2 Specification of prior densities

As explained in the main text, we first estimate the SQVAR model's parameters for U.S. data. We do so using the same model specification (i.e., variables, deterministic terms, number of lags and zero restrictions). Next, we let these estimates inform the euro area parameters' priors. We are thus taking advantage of decades of data available for the U.S. between 1973Q1 and 2022Q4. Both the U.S. and euro area economies are advanced, market-based economies with institutional similarities along many dimensions.

A.2.1 Priors for U.S. data

We need to specify the prior parameters $\underline{\mu}_{\beta,i}^{US}$ $\underline{\Sigma}_i^{US}$, $\underline{\alpha}_{\sigma,i}^{US}$, $\underline{\zeta}_{\sigma,i}^{US}$, $\underline{\alpha}_{\lambda,i}^{US}$, and $\underline{\zeta}_{\lambda,i}^{US}$. For U.S. data, we keep the prior parameters homogeneous across quantiles. We have therefore dropped a potential dependence on γ.

We employ a Minnesota prior for the vector of coefficients β_i^{US} (see, e.g., Litterman, 1986, Luetkepohl, 2005, p. 225, Giannone et al., 2015). This means that the prior density is Gaussian, and pointing to a persistent autoregressive process of order one. Specifically, we set the coefficient in β_i^{US} referring to variable i's own first lag equal to either 0.9 or 1, depending on the variable. For the CISS, the financial cycle, and the real GDP growth rate, the own-lag coefficient is set to 0.9; for CPI inflation and the Federal Funds Rate the coefficient is set to one. All other elements of β_i^{US} are given a prior mean of zero.

We further specify the Minnesota prior's covariance matrix $\underline{\Sigma}_{\beta,i}^{US}$ as diagonal, with $\underline{\sigma}_{\beta,ij,l}^{US}$ the element corresponding to the lth lag of the jth endogenous variable in equation i. The diagonal

elements are given by

$$\begin{aligned}
\underline{\sigma}^{US}_{\beta,ij,l} &= \phi_0^2 && \text{if } i=j, l=0 \\
\underline{\sigma}^{US}_{\beta,ij,l} &= \left(\frac{\phi_0}{l^{\phi_3}}\right)^2 && \text{if } i=j, l>0 \\
\underline{\sigma}^{US}_{\beta,ij,l} &= \left(\phi_0\phi_1\frac{\hat{\sigma}_i}{\hat{\sigma}_j}\right)^2 && \text{if } i\neq j, l=0 \\
\underline{\sigma}^{US}_{\beta,ij,l} &= \left(\frac{\phi_0\phi_1}{l^{\phi_3}}\frac{\hat{\sigma}_i}{\hat{\sigma}_j}\right)^2 && \text{if } i\neq j, l>0 \\
\underline{\sigma}^{US}_{\beta} &= (\phi_0\phi_2)^2 && \text{otherwise,}
\end{aligned}$$

where ϕ_0 is a general tightness parameter, ϕ_1 a tightness parameter on endogenous variables other than variable i, ϕ_2 a tightness parameter on exogenous variables and deterministic terms, and ϕ_3 a tightness parameter controlling the importance of lags of endogenous variables. We choose $\phi_0 = 0.2$, $\phi_1 = 0.5$, $\phi_2 = 10^5$, and $\phi_3 = 1$. These are common choices in the literature (see, e.g., Litterman, 1986). Parameter $\hat{\sigma}_i$ denotes the standard error of the residuals from a univariate quantile autoregression on endogenous variable i at the median. Finally, we set $\underline{\alpha}^{US}_{\sigma,i} = \underline{\zeta}^{US}_{\sigma,i} = 0.01$, corresponding to a non-informative prior for the scale parameter σ. We also set $\underline{\alpha}^{US}_{\lambda,i} = 3$ and $\underline{\zeta}^{US}_{\lambda,i} = 6$, implying a prior mean and a prior standard deviation of 3 for λ_i.

A.2.2 Priors for euro area data

We set the euro area prior parameters for $\beta^{EA}_i(\gamma)$ to match the corresponding posterior moments obtained from U.S. data. Specifically,

$$\begin{aligned}
\underline{\mu}^{EA}_{\beta,i}(\gamma) &= \frac{1}{N^S}\sum_{s=1}^{N^S}\hat{\beta}^{US}_{i,s}(\gamma) \\
\underline{\Sigma}^{EA}_{\beta,i}(\gamma) &= \frac{1}{N^S}\sum_{s=1}^{N^S}\left(\hat{\beta}^{US}_{i,s}(\gamma) - \underline{\mu}^{EA}_{\beta,i}(\gamma)\right)^2,
\end{aligned}$$

where $\hat{\beta}^{US}_{i,s}$ are the N^S posterior draws of β^{US}_i. All other euro area hyperparameters are given values identical to their U.S. counterparts. Specifically, $\underline{\alpha}^{EA}_{\sigma,i} = \underline{\zeta}^{EA}_{\sigma,i} = 0.01$, $\underline{\alpha}^{EA}_{\lambda,i} = 3$, and $\underline{\zeta}^{EA}_{\lambda,i} = 6$.

A.3 Posterior density for λ

This section derives the fourth step of the Gibbs sampler in Section A.1. This step is introduced to estimate a tightness parameter that determines the weight given to the U.S. parameter estimates in forming the priors for estimating the euro area model. Allowing the data to help decide on the tightness of the prior density across quantiles and variables appears particularly appropriate in our case, as we have no reliable prior knowledge of how informative the Minnesota prior is for the parameters of the U.S. model at any given quantile, nor how informative the U.S. posterior density is for the parameters of the euro area model. Bayesian updating of the tightness parameter through a hyper-prior is a common solution, for example, in the literature on shrinkage in Bayesian regression models (see e.g. Huber and Feldkircher, 2019 and Korobilis and Pettenuzzo, 2019). In addition, such updating is common in the analysis of sequential medical trials (see, e.g., Ibrahim et al., 2015 and Ibrahim and Chen, 2000).

To arrive at the conditional posterior distribution for λ, again dropping subscripts γ and i for clarity, we start by writing out the kernel of the joint posterior distribution, $\mathcal{P}(\cdot)$, with the terms relating to λ,

$$\mathcal{P}(\lambda|\cdot) \propto |\lambda\underline{\Sigma}_\beta|^{-\frac{1}{2}} \exp\left\{-\frac{1}{2}\left(\beta-\underline{\mu}_\beta\right)'\lambda^{-1}\underline{\Sigma}_\beta^{-1}\left(\beta-\underline{\mu}_\beta\right)\right\} \times \lambda^{-\underline{\alpha}_\lambda-1}\exp\left\{-\underline{\zeta}_\lambda\lambda^{-1}\right\},$$

where the first term comes from the normally distributed prior for β and the second term from the inverse-gamma prior distribution for λ. Rewriting the above expression, we obtain

$$\begin{aligned}\mathcal{P}(\lambda|\cdot) &\propto \lambda^{-\underline{\alpha}_\lambda-\frac{\tilde{k}}{2}-1}\exp\left\{-\lambda^{-1}\left(\frac{1}{2}\left(\beta-\underline{\mu}_\beta\right)'\underline{\Sigma}_\beta^{-1}\left(\beta-\underline{\mu}_\beta\right)+\underline{\zeta}_\lambda\right)\right\}\\ &\propto IG\left(\bar{\alpha}_\lambda,\bar{\zeta}_\lambda\right),\end{aligned}$$

where $\bar{\alpha}_\lambda = \underline{\alpha}_\lambda + \frac{\tilde{k}}{2}$ and $\bar{\zeta}_\lambda = \underline{\zeta}_\lambda + \frac{1}{2}\left(\beta-\underline{\mu}_\beta\right)'\underline{\Sigma}_\beta^{-1}\left(\beta-\underline{\mu}_\beta\right)$, and where $\tilde{k}$ denotes the number of regressors. As a result, we can immediately draw λ from its posterior distribution conditional on a posterior draw of β.

B Technical details

B.1 Quantile impulse response functions

This section presents the simulation algorithm used to obtain quantile impulse response functions (QIRFs). For a given set of coefficients, we require two sets of conditional distributions to compare: First, we require the conditional forecast distribution of the data in a baseline scenario without an initial shock. Second, we require the conditional forecast distribution of the data in a counterfactual scenario in which a single shock arrives in the first forecasting period. The QIRFs are obtained as the difference between the latter and the former distribution.

B.1.1 Notation

Throughout this section, we represent the SQVAR(p) as

$$x_t = \omega(\gamma) + A_0(\gamma)x_t + \sum_{j=1}^{p} A_j(\gamma)x_{t-j} + B(\gamma)d_t + \sum_{j=0}^{p} C_j(\gamma)z_{t-j} + \varepsilon_t^{\gamma}, \tag{B.1}$$

for a given $\gamma \equiv [\gamma_1, \ldots, \gamma_n]'$, and recall the identifying assumption $Q_\gamma\left(\varepsilon_t^{\gamma}|\Omega_t\right) = 0_{n\times 1}$. Similarly, each of the r exogenous variables is modeled as a univariate quantile autoregressive (QAR) process,

$$z_{vt} = \mathcal{W}_v(\gamma_v^*) + \sum_{j=1}^{p} \mathcal{A}_{j,v}(\gamma_v^*)z_{v,t-j} + \mathcal{B}_v(\gamma_v^*)d_t + \xi_{vt}^{\gamma_v^*}, \tag{B.2}$$

for $\gamma^* \equiv [\gamma_1^*, \ldots, \gamma_v^*, \ldots, \gamma_r^*]'$. To establish notation for the remainder of this section, we let H denote the forecast horizon, o the forecast origin, M the number of posterior draws required for posterior inference of the QIRFs, and S the number of forward simulations for each posterior draw. We assume that $\mathcal{G} = \{0.05, 0.10, \ldots, 0.90, 0.95\}$ is a sufficiently large set of $q = 19$ quantiles distributed symmetrically around the median. We obtain $N^S = 2,500$ draws of each $\beta_i(\gamma)$, after discarding a burn-in sample of $N^B = 2,500$.

B.1.2 Algorithm

The algorithm proceeds as follows.

1. **Obtain posterior draws.** Obtain and store N^S posterior draws for all the SQVAR's parameters in (B.1) and (B.2) at all quantiles, see Appendix A.1. We store them in a four-dimensional array of dimensions $[n+r] \times [p(n+r)+r+1+k] \times q \times N^S$.

2. **Choose forecast origin.** Fix the initial conditions for the endogenous variables $x_{o-(p-1):o}$ and exogenous variables $z_{o-(p-1):o}$. We use the unconditional median over the estimation sample for all variables.

3. Set $m = 1$.

   3.1. **Draw parameters.** Let $\hat{\beta}^{(m)}$ be a random draw from the set of N^S posterior draws, and $\hat{\beta}_i^{(m)}(\check{\gamma})$ the subset of parameters corresponding to the posterior draw of β_i for some quantile $\check{\gamma}$.

   3.2. Let $\hat{\epsilon}_{o+1}$ be an $n \times 1$ vector of zeros.

   3.3. Set $s = 1$.

      3.3.1. Set $h = 1$.

         3.3.1.1. **Draw quantiles at random.** Obtain n random draws from the uniform distribution $\mathrm{U}(0,1)$ and map them to the corresponding quantiles in $\mathcal{G}$ based on proximity. Stack the mapped quantiles in the $n \times 1$ vector ϱ. Define the $r \times 1$ vector ϱ^* in a similar fashion.

         3.3.1.2. **Set up SQVAR system matrices.** Let $f_{A_j}\left(\hat{\beta}_i^{(m)}(\check{\gamma})\right)$ be a mapping from posterior draw $\hat{\beta}_i^{(m)}(\check{\gamma})$ to the ith row of A_j in (B.1). Define similar mappings for the remaining matrix coefficients. Using these mappings, stack the variable-

specific posterior draws into matrices of quantile coefficients, such that

$$\tilde{A}_j^{o+h} = \begin{bmatrix} f_{A_j}\left(\hat{\beta}_1^{(m)}(\varrho_1)\right) \\ \vdots \\ f_{A_j}\left(\hat{\beta}_i^{(m)}(\varrho_i)\right) \\ \vdots \\ f_{A_j}\left(\hat{\beta}_n^{(m)}(\varrho_n)\right) \end{bmatrix} \qquad \tilde{\omega}^{o+h} = \begin{bmatrix} f_{\omega}\left(\hat{\beta}_1^{(m)}(\varrho_1)\right) \\ \vdots \\ f_{\omega}\left(\hat{\beta}_i^{(m)}(\varrho_i)\right) \\ \vdots \\ f_{\omega}\left(\hat{\beta}_n^{(m)}(\varrho_n)\right) \end{bmatrix}$$

$$\tilde{C}_j^{o+h} = \begin{bmatrix} f_{C_j}\left(\hat{\beta}_1^{(m)}(\varrho_1)\right) \\ \vdots \\ f_{C_j}\left(\hat{\beta}_i^{(m)}(\varrho_i)\right) \\ \vdots \\ f_{C_j}\left(\hat{\beta}_n^{(m)}(\varrho_n)\right) \end{bmatrix} \qquad \tilde{B}^{o+h} = \begin{bmatrix} f_{B}\left(\hat{\beta}_1^{(m)}(\varrho_1)\right) \\ \vdots \\ f_{B}\left(\hat{\beta}_i^{(m)}(\varrho_i)\right) \\ \vdots \\ f_{B}\left(\hat{\beta}_n^{(m)}(\varrho_n)\right) \end{bmatrix}$$

for $j = 0, \ldots, p$ and $h = 1, \ldots, H$. Define the corresponding matrices for the exogenous variables analogously using ϱ^*, resulting in matrices $\tilde{\mathcal{W}}_v^{o+h}$, $\tilde{\mathcal{A}}_{j,v}^{o+h}$ and $\tilde{\mathcal{B}}_v^{o+h}$.

3.3.1.3. **Iterate exogenous variables forward.** Compute the conditional forecast of each of the r exogenous variables, $z_{o+h}^{(s)}$, using (B.2) and the relevant quantile coefficients determined in the previous step as

$$z_{v,o+h}^{(s)} = \tilde{\mathcal{W}}_v^{o+h} + \sum_{j=1}^{P} \tilde{\mathcal{A}}_{j,v}^{o+h} z_{v,o+h-j}^{(s)} + \tilde{\mathcal{B}}_v^{o+h} d_{t+h}.$$

3.3.1.4. **Iterate endogenous variables forward.** Compute the conditional forecast of $x_{o+h}^{(s)}$ using (B.1) and the relevant quantile coefficients determined in step 3.3.1.2 as

$$x_{o+h}^{(s)} = \left(I - \tilde{A}_0^{o+h}\right)^{-1} \begin{bmatrix} \tilde{\omega}^{o+h} + \sum_{j=1}^{P} \tilde{A}_j^{o+h} x_{o+h-j}^{(s)} \\ + \tilde{B}^{o+h} d_{t+h} + \sum_{j=0}^{P} \tilde{C}_j^{o+h} z_{o+h-j}^{(s)} + \hat{\epsilon}_{o+h} \end{bmatrix}$$

3.3.1.5. If $h < H$, set $h = h + 1$ and return to step 3.3.1.1.

3.3.2. If $s < S$, set $s = s + 1$ and return to step 3.3.1.

3.4. **Obtain predicted quantiles.** Let $\check{\mathbf{x}}_{o+h} = \{x_{o+h}^{(s)}\}_{s=1}^{S}$ be the set of S simulated forecasts of x_{o+h}. Compute the γth conditional quantile forecast of $x_{i,o+h}$ as

$$Q_\gamma\left(x_{i,o+h}|\Omega_o\right) = Q_\gamma\left(\check{\mathbf{x}}_{i,o+h}\right),$$

where $Q_\gamma\left(\cdot|\Omega_o\right)$ is the γth quantile conditional on the information set Ω_o, and letting $Q_\gamma\left(\cdot\right)$ denote the empirical quantile function. This concludes the baseline (no shock) forward simulations.

3.5. **Choose the shock of interest.** Let $\mathcal{S}$ be an $n \times 1$ selection vector picking the endogenous variable i to be shocked. (That is, the ith element of $\mathcal{S}$ is 1 and 0 otherwise.) Redefine $\hat{\epsilon}_{o+h} = \psi\mathcal{S}$, where ψ is a scalar. A common choice of magnitude ψ is the estimated standard deviation of quantile shocks obtained at the median. Repeat steps 3.3 - 3.4 to obtain the quantile projection conditional on the shock, $Q_\gamma\left(x_{i,o+h}|\Omega_o, \psi\right)$.

3.6. **Compute the γth quantile impulse response function** as

$$\iota_{\gamma,i,o+h}^{(m)} = Q_\gamma\left(x_{i,o+h}|\Omega_o, \psi\right) - Q_\gamma\left(x_{i,o+h}|\Omega_o\right)$$

3.7. If $m < M$, set $m = m + 1$ and return to step 3.2.

Posterior inference of the QIRF of the conditional quantile γ of variable i in period $o+h$ is obtained from the sequence $\left\{\iota_{\gamma,i,o+h}^{(m)}\right\}_{m=1}^{M}$.

B.2 Simulation algorithm for downside risk measures

We obtain measures of downside risks to economic growth between o and $o+h$ by reusing the simulation algorithm in Section B.1, but now replace steps 3.4-3.6 with the following steps.

3.4. For each forecast horizon, compute the $o+h$ growth shortfall as

$$\text{GS}_{o,o+h}^{\tau,(m)} = \frac{1}{S}\sum_{s=1}^{S} \tilde{y}_{o+h}^{(s)} \cdot 1\{\tilde{y}_{o+h}^{(s)} < \tau\},$$

where $\tilde{y}_{o+h}^{(s)}$ denotes a simulated value for quarterly real GDP growth at time $o+h$.

3.5. Compute the final time-o downside risk measure as averages across simulations

$$\text{AGS}_{o,o+1:o+h}^{\tau,(m)} = \frac{1}{H}\sum_{h=1}^{H} \text{GS}_{o,o+h}^{\tau,(m)}$$

Posterior inference is obtained from the sequence $\left\{\text{AGS}_{o,o+1:o+h}^{\tau,(m)}\right\}_{m=1}^{M}$. The above steps can similarly be used to compute average growth longrise.

B.3 Counterfactual scenarios

Rather than moving through the tree of potential future values of x_{t+h} completely at random, as done in Web Appendix B.2, we may sometimes wish to consider only a subset of paths, or even just one path, in isolation. Such paths can also be thought of as a 'counterfactual scenario,' or model-based thought experiment, that conditions on an arbitrary but fixed sequence of future shocks.

To this effect, let Γ^* denote a design matrix of size $H \times (n + r)$. Each element of Γ^* is either empty or in the interval $(0, 1)$. Any non-empty hth element of the ith column designates the quantile path to be traveled by variable i in period h in all S simulations. An empty element means that the path is chosen at random. The matrix Γ^* can then be readily applied in Step 3.3.1.1 in the simulation algorithm of Section B.1 to obtain density forecasts in a counterfactual scenario.

An illustration of this principle is given in Figure B.1. There, a single variable, y, is projected forward for $H = 3$ periods using two estimated quantiles, $\gamma \in \{\text{u}, \text{d}\}$. An unrestricted projection as in Figure B.1a yields a total of $2^3 = 8$ unique paths for y to travel along. Consider now the counterfactual, in which we require y to initially increase, then decrease, and then finally increase again. This maps to the path satisfying $\Gamma^* = \{\text{u}, \text{d}, \text{u}\}'$, highlighted by the red dashed lines in Figure B.1b.

Instead of a fully restricted tree, as illustrated above, one may also consider a partially restricted tree. In a partially restricted tree, the quantile paths are only fixed for some of the periods or variables. In the example above, one may, for instance, require that the chosen quantile from period 1 to 2 is always $\{\text{d}\}$, while leaving the remaining branches unrestricted. In this case, the total number of paths that can be traveled equals four $\left(Q^{\text{u,d,u}}, Q^{\text{u,d,d}}, Q^{\text{d,d,u}}, Q^{\text{d,d,d}}\right)$.

Figure B.1: Illustration of counterfactual scenario analysis through quantile restrictions

Notes: Filled blue lines indicate unrestricted paths, red dashed lines restricted paths, and transparent blue lines the paths excluded by the imposed restrictions.

(a) Uncrestricted tree

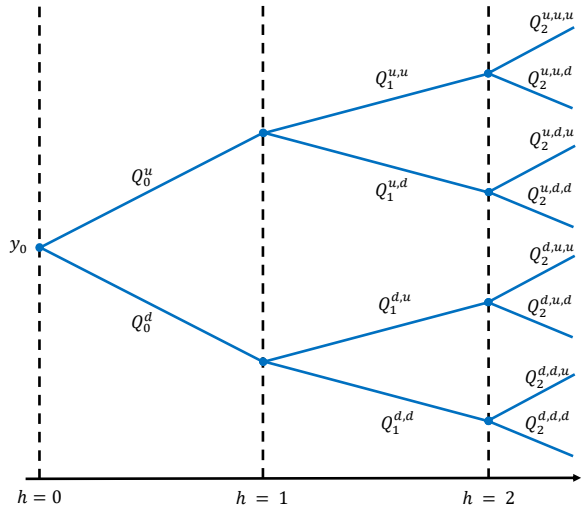

(b) Fully restricted tree

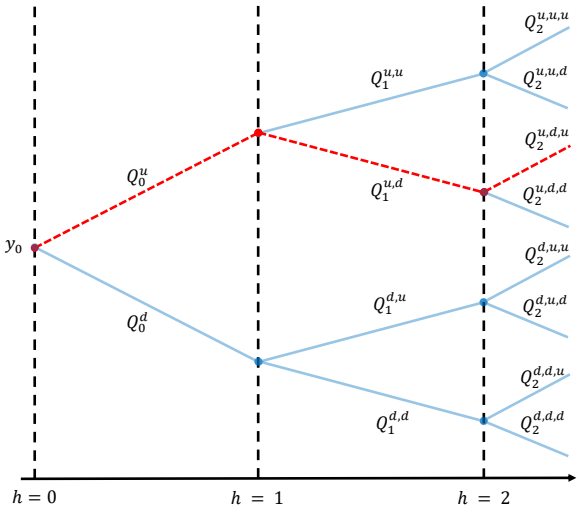

C Data plots

Figure C.1: Euro area and U.S. time series

Notes: Annualised inflation and growth rates are calculated as 400 times the log-difference between quarterly averages.
Sources: European Central Bank, U.S. Bureau of Labor Statistics, U.S. Bureau of Economic Analysis, Board of Governors of the Federal Reserve System, LSEG, Haver Analytics, and authors' calculations.

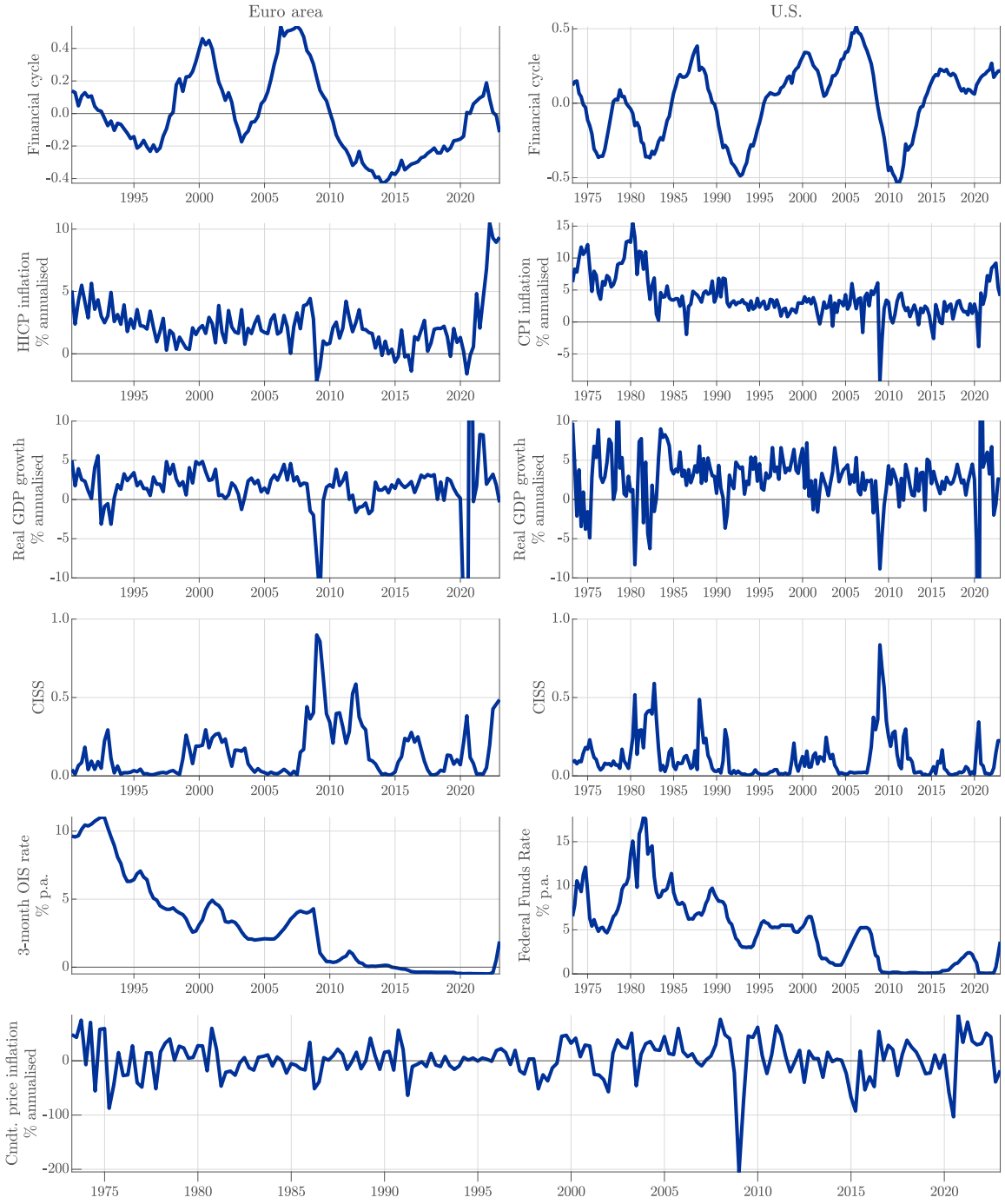

D Euro area posterior estimates

Figure D.1: Posterior inference for the euro area, $\omega(\gamma)$

Posterior mean and 95% credible intervals obtained from 2,500 posterior draws. Least squares estimates (in red) for the conditional mean are provided for comparison.

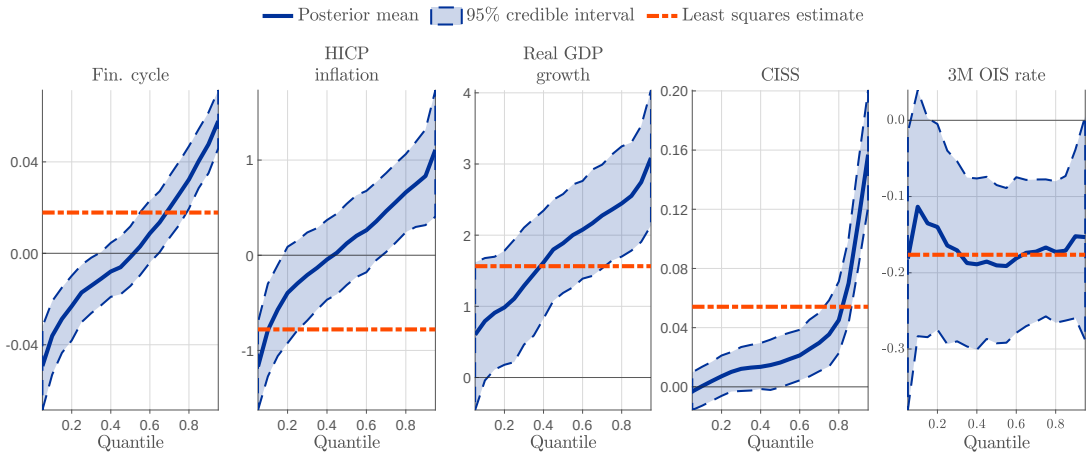

Figure D.2: Posterior inference for the euro area, $A_0(\gamma)$

Posterior mean and 95% credible intervals are obtained from 2,500 posterior draws. Least squares estimates are provided for comparison.

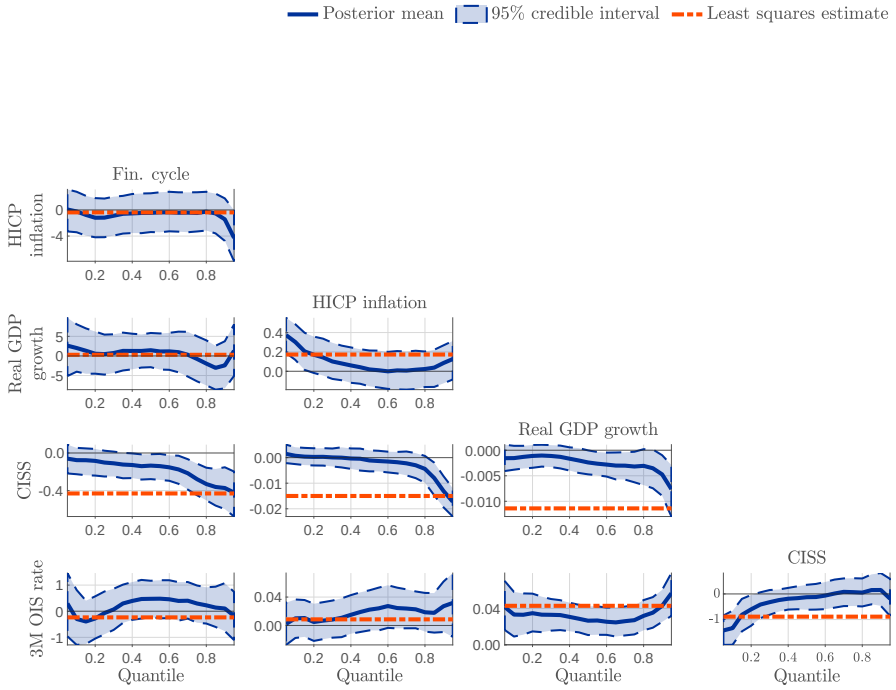

Figure D.3: Posterior inference for the euro area, $A_1(\gamma)$

Posterior mean and 95% credible intervals are obtained from 2,500 posterior draws. Least squares estimates are provided for comparison.

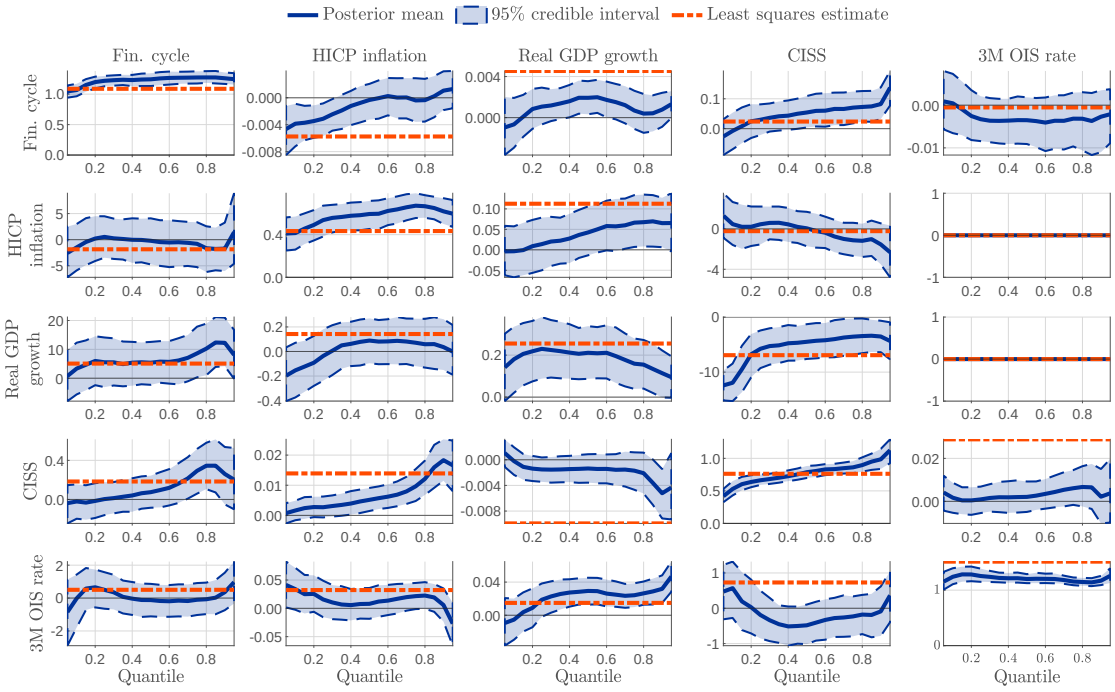

Figure D.4: Posterior inference for the euro area, $A_2(\gamma)$

Posterior mean and 95% credible intervals are obtained from 2,500 posterior draws. Least squares estimates are provided for comparison.

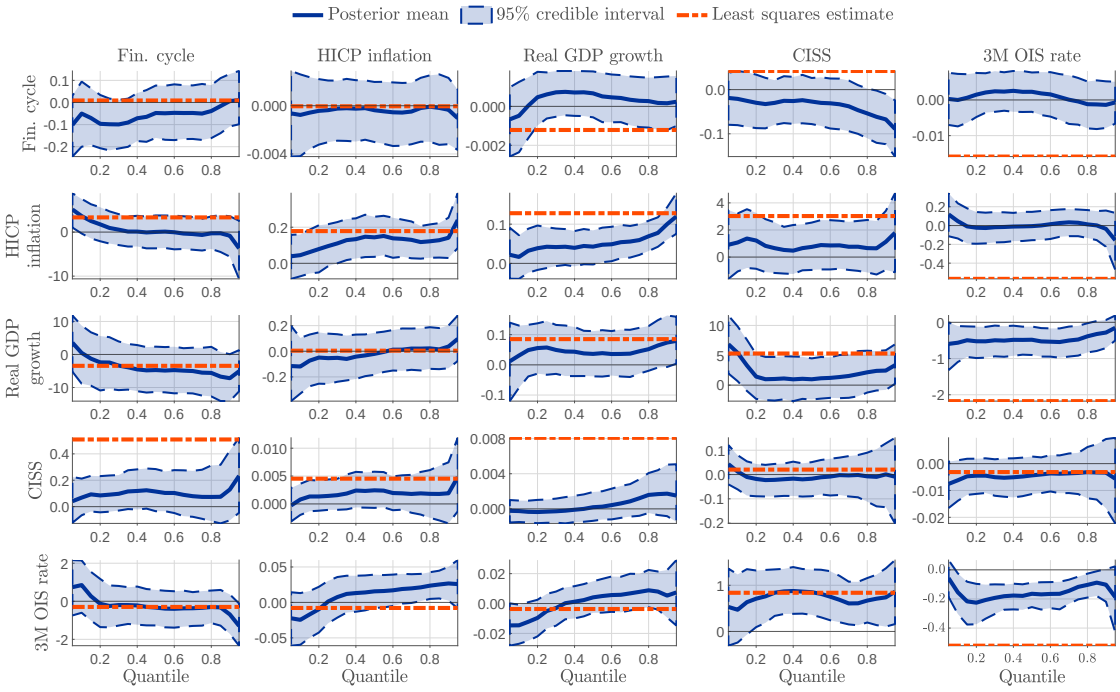

Figure D.5: Posterior inference for the euro area, $A_3(\gamma)$

Posterior mean and 95% credible intervals are obtained from 2,500 posterior draws. Least squares estimates are provided for comparison.

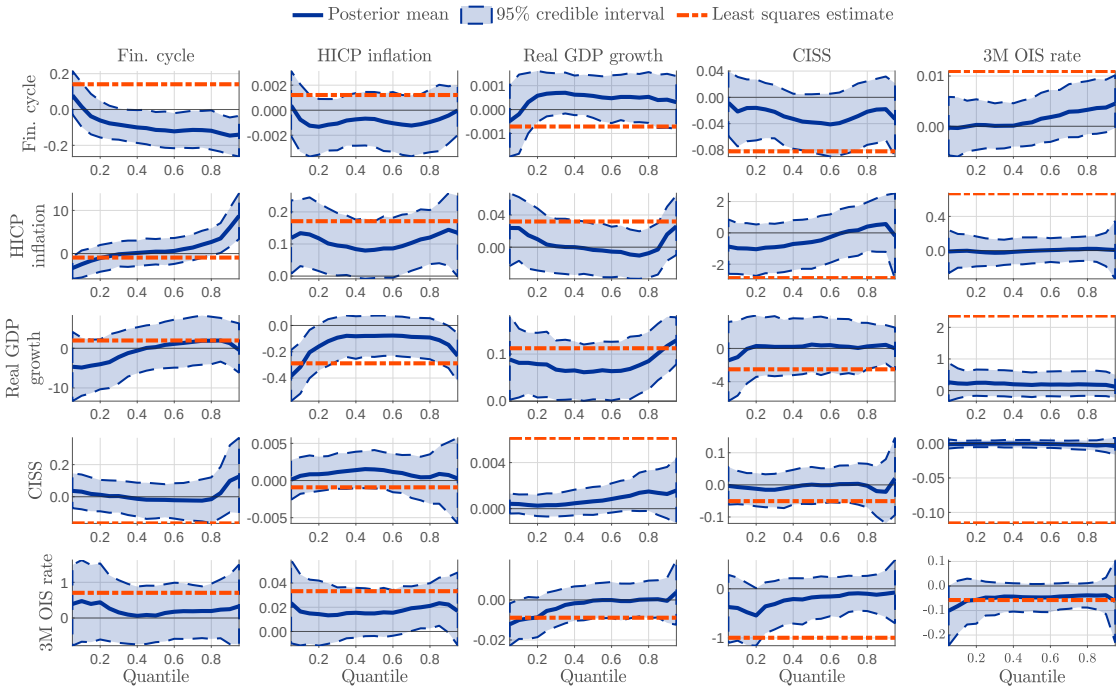

Figure D.6: Posterior inference for the euro area, $A_4(\gamma)$

Posterior mean and 95% credible intervals are obtained from 2,500 posterior draws. Least squares estimates are provided for comparison.

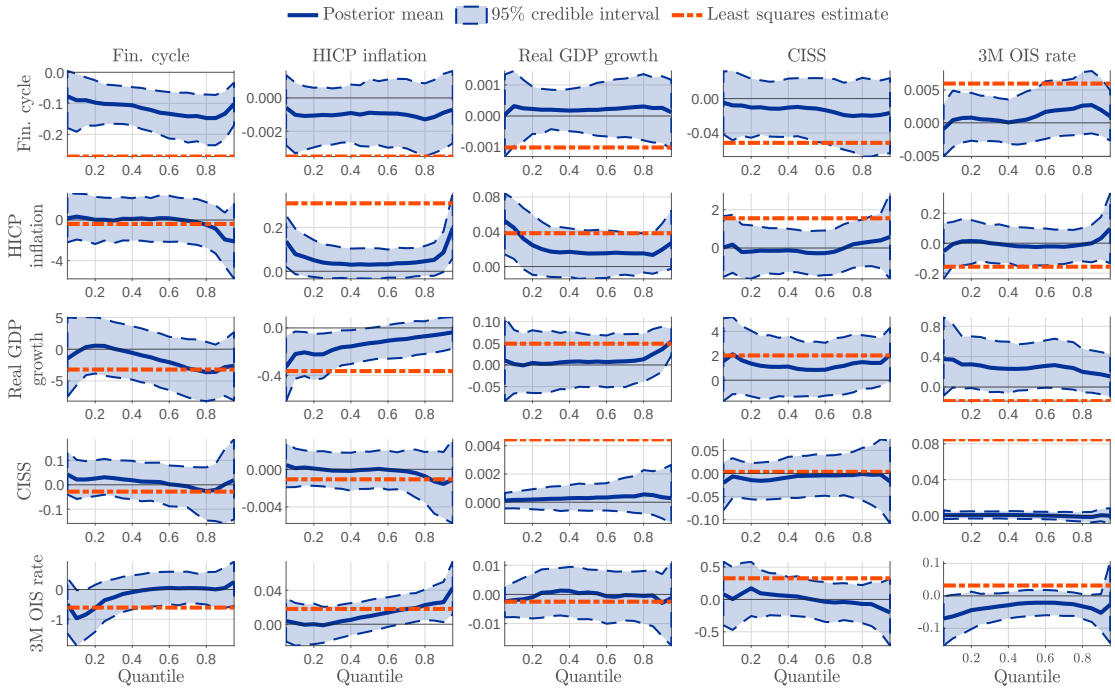

Figure D.7: Posterior inference for the euro area exogenous variables, $C(\gamma)$

Posterior mean and 95% credible intervals are btained from 2,500 posterior draws. Least squares estimates are provided for comparison.

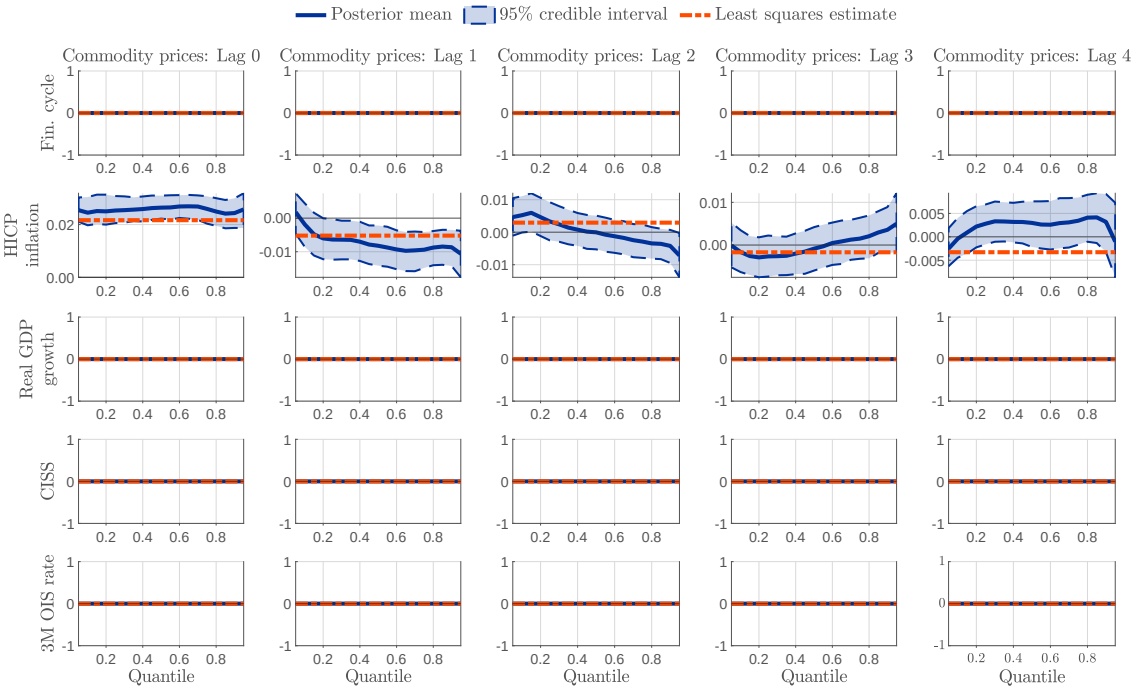

Figure D.8: Posterior inference for the euro area dummy variables, $B(\gamma)$

Posterior mean and 95% credible intervals are obtained from 2,500 posterior draws. Least squares estimates are provided for comparison.

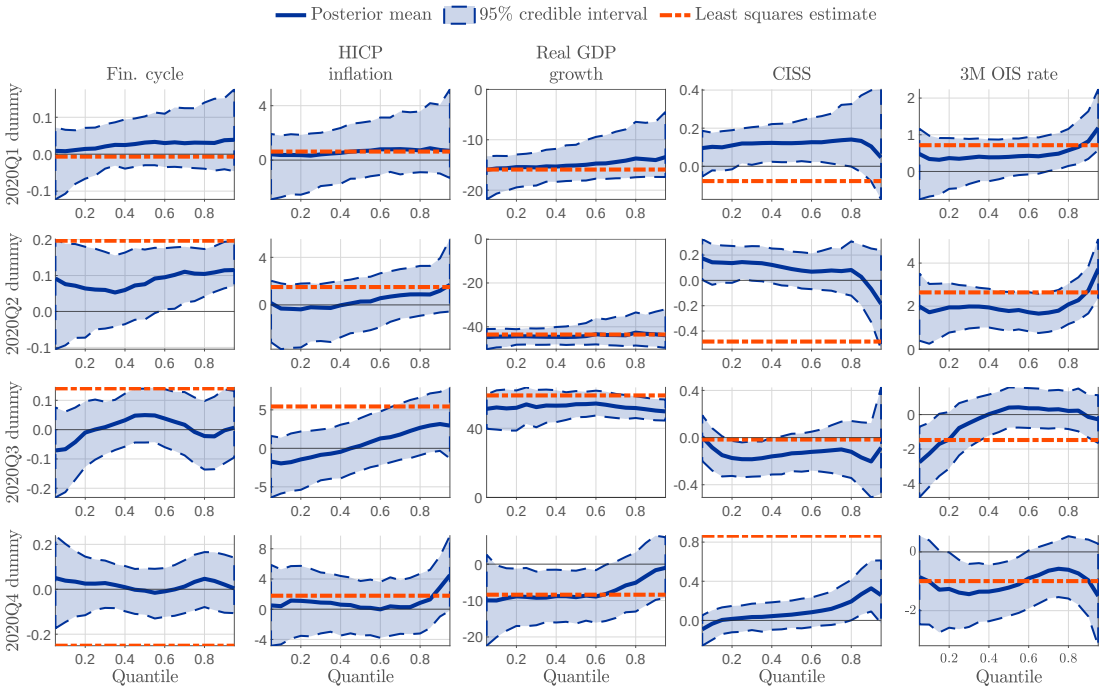

Figure D.9: Posterior means for the euro area tightness parameter, $\lambda_i(\gamma)$

Posterior mean estimates of $\lambda_i(\gamma)$ are obtained from 2,500 posterior draws.

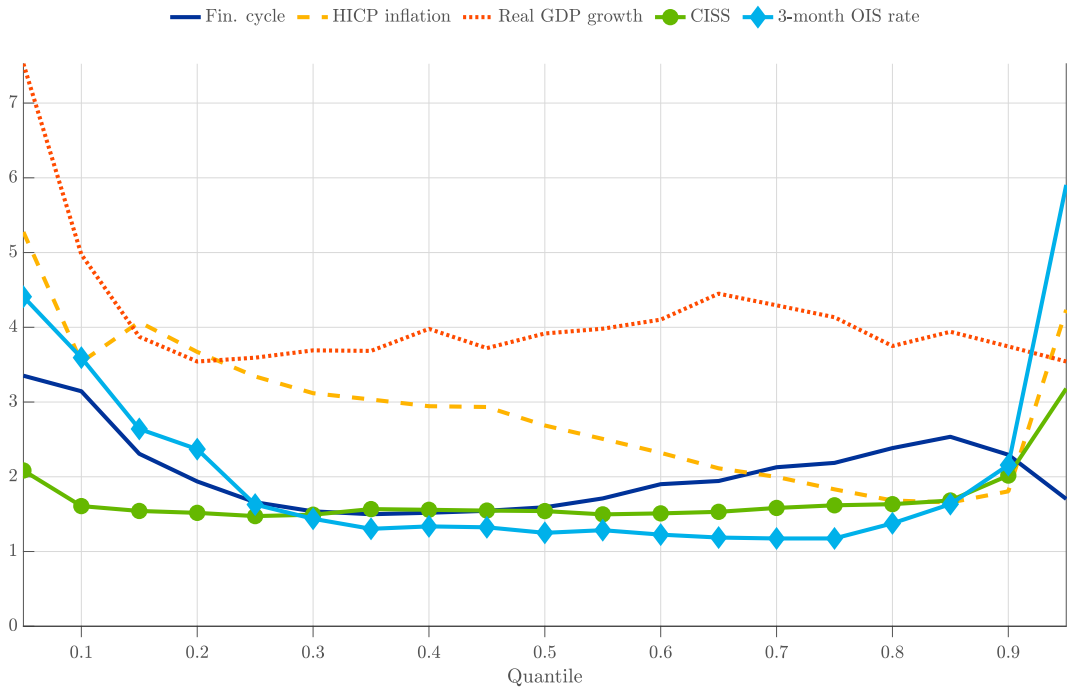

Figure D.10: Quantile impulse response functions for the euro area

Impulse response functions implied by the posterior estimates reported in Figures D.1-D.8. Based on 400 draws from the posterior distribution and 20.000 forward simulations of the conditional distribution for each draw. Shocks are equal to the standard deviation of residuals from the median quantile regression of the respective variables. Variables are ordered financial cycle (respective first row), HICP inflation (second row), GDP growth (third row), CISS (fourth row), and the 3-month OIS rate (fifth row). Credible intervals are dashed and at a 95% level. Estimation sample is 1990Q1 to 2022Q4.

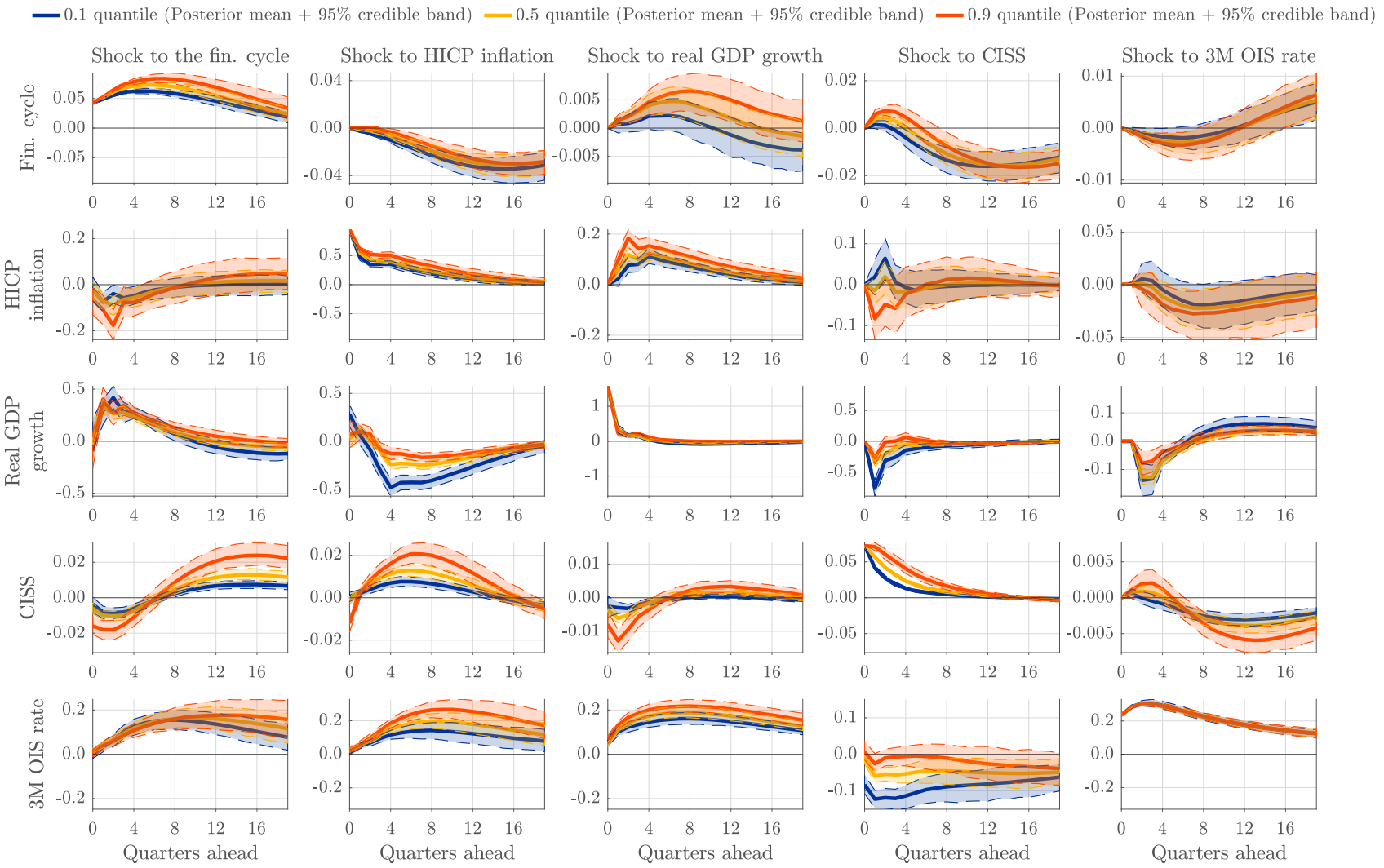

E U.S. posterior estimates

Figure E.1: Posterior inference for the U.S. , $\omega(\gamma)$

Posterior mean and 95% credible intervals are obtained from 2,500 posterior draws. Least squares estimates (in red) for the conditional mean are provided for comparison.

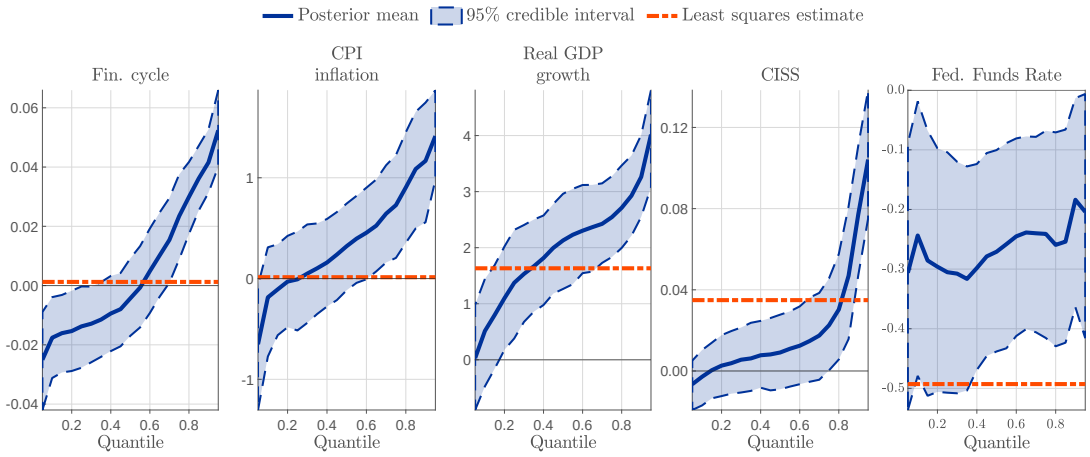

Figure E.2: Posterior inference for the U.S., $A_0(\gamma)$

Posterior mean and 95% credible intervals are obtained from 2,500 posterior draws. Least squares estimates for the conditional mean are provided for comparison.

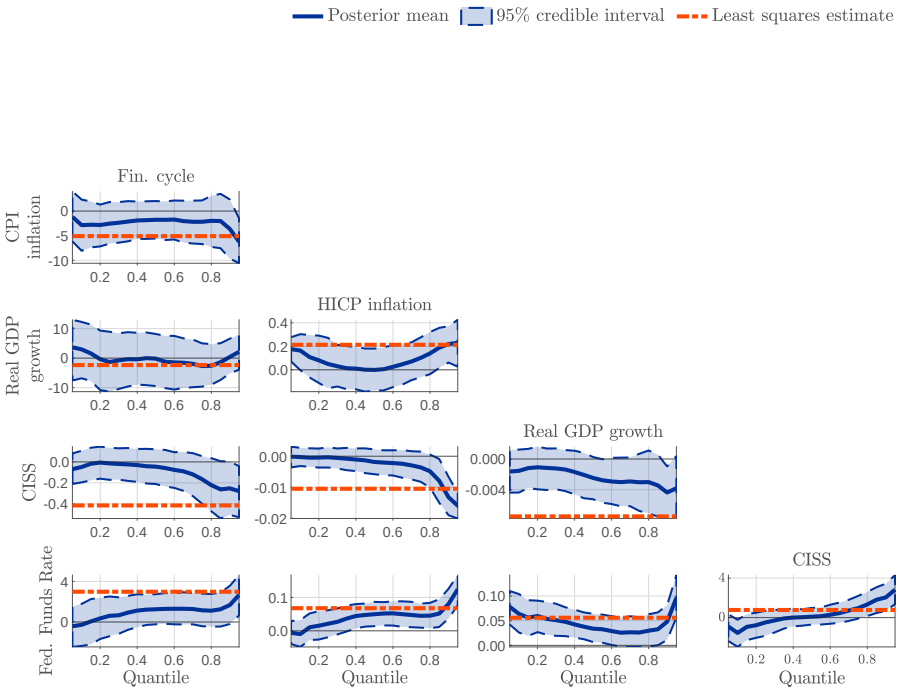

Figure E.3: Posterior inference for the U.S., $A_1(\gamma)$

Posterior mean and 95% credible intervals are obtained from 2,500 posterior draws. Least squares estimates are for comparison.

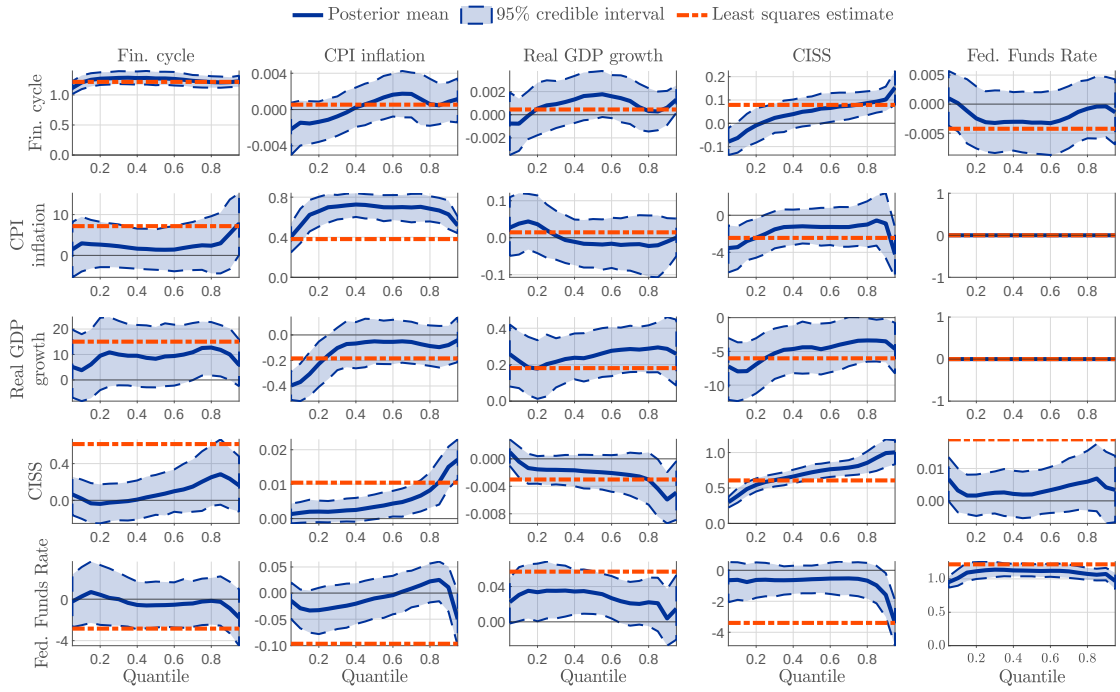

Figure E.4: Posterior inference for the U.S., $A_2(\gamma)$

Posterior mean and 95% credible intervals are obtained from 2,500 posterior draws. Least squares estimates are for comparison.

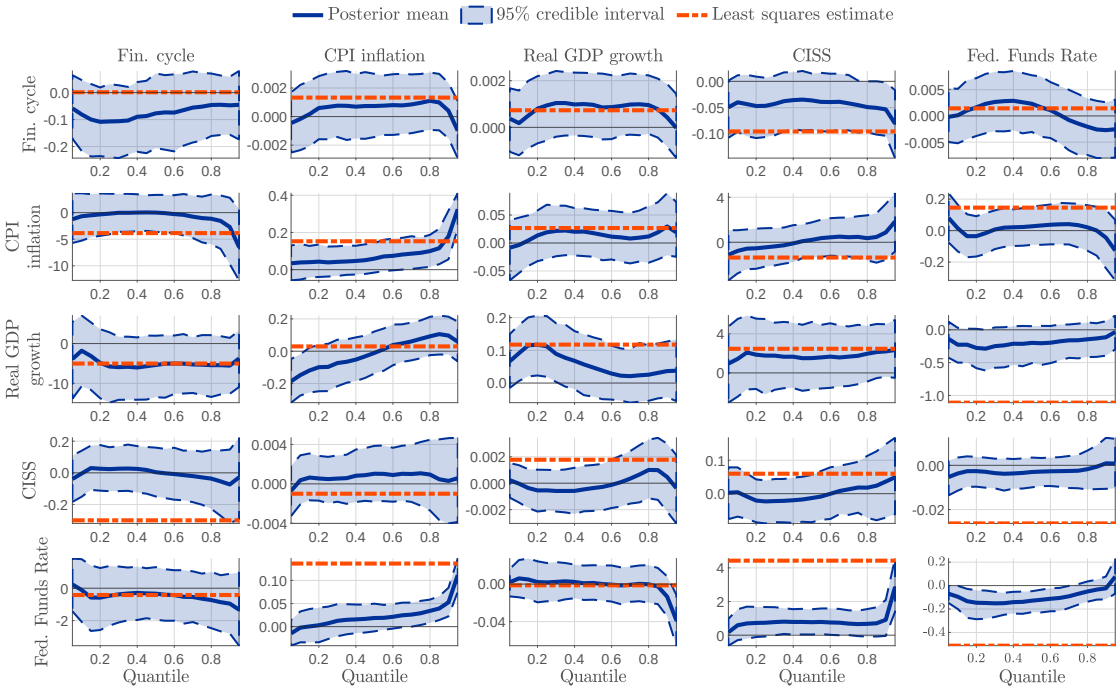

Figure E.5: Posterior inference for the U.S., $A_3(\gamma)$

Posterior mean and 95% credible intervals are obtained from 2,500 posterior draws. Least squares estimates are provided for comparison.

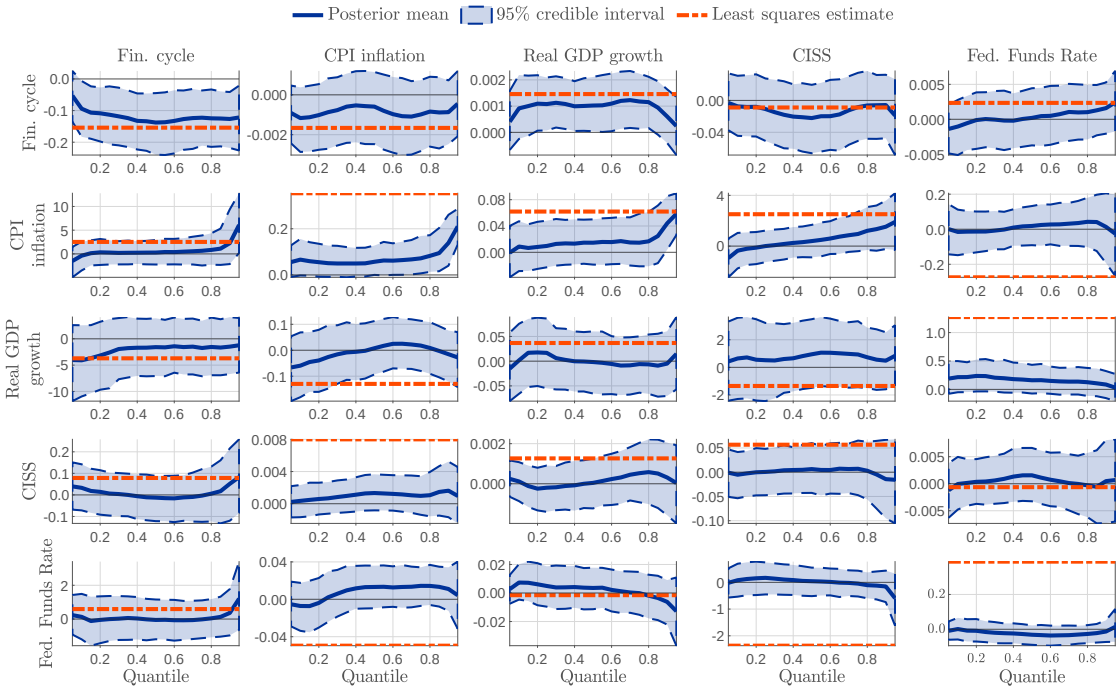

Figure E.6: Posterior inference for the U.S., $A_4(\gamma)$

Posterior mean and 95% credible intervals are obtained from 2,500 posterior draws. Least squares estimates are provided for comparison.

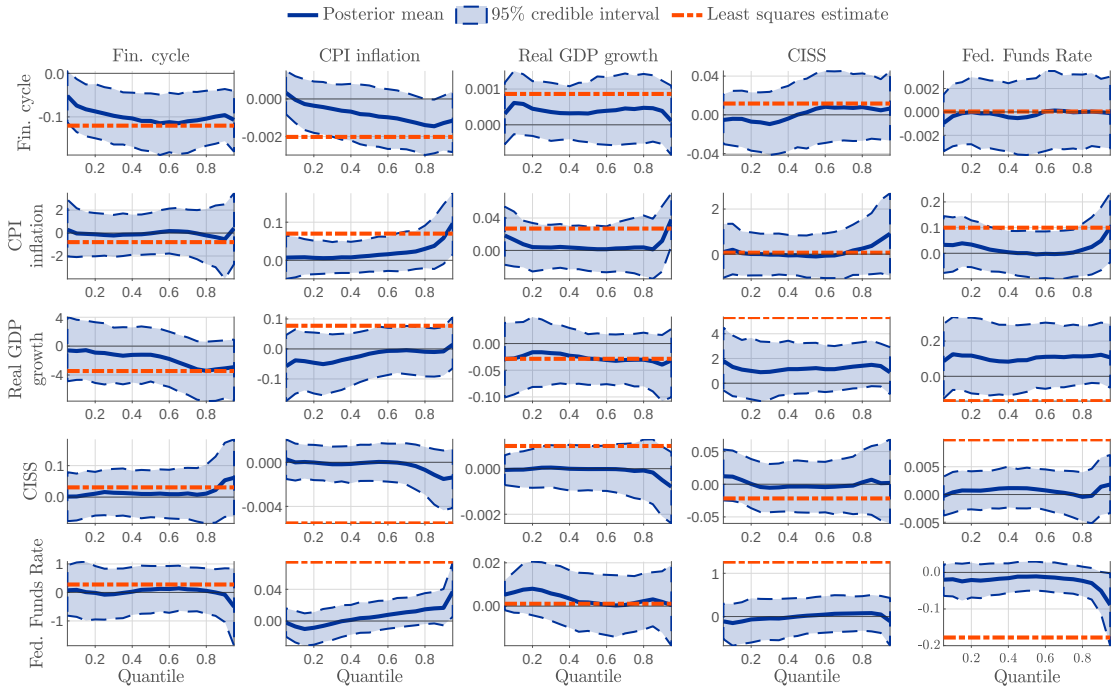

Figure E.7: Posterior inference for the U.S. exogenous variables, $C(\gamma)$

Posterior mean and 95% credible intervals are obtained from 2,500 posterior draws. Least squares estimates are provided for comparison.

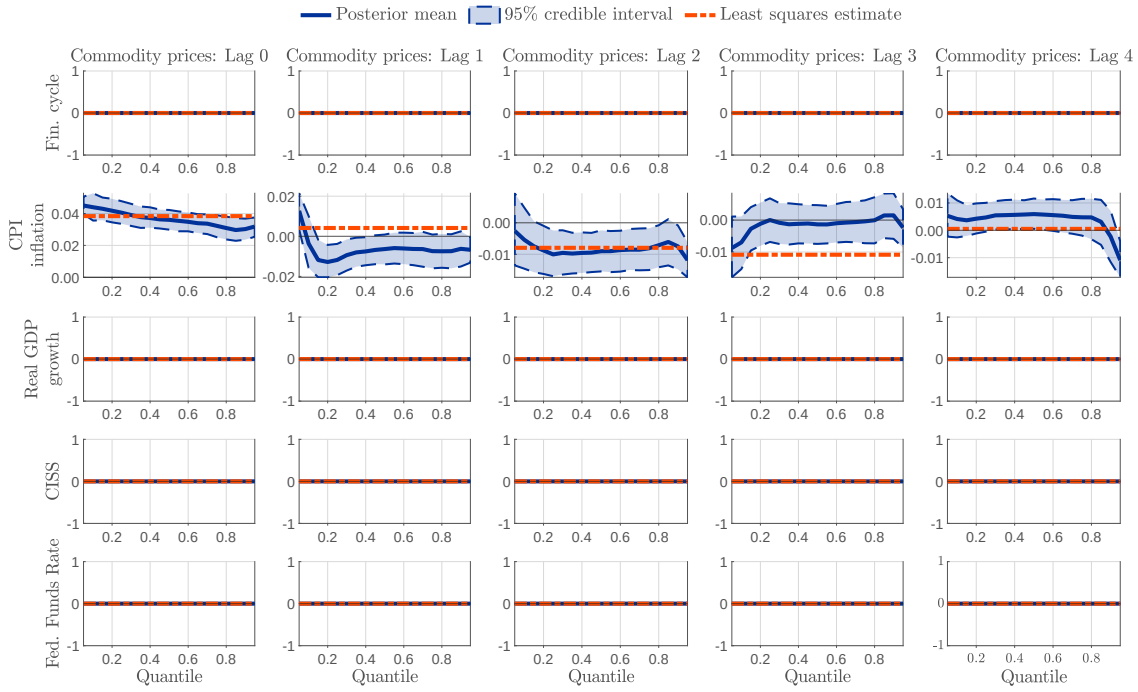

Figure E.8: Posterior inference for the U.S. dummy variables, $B(\gamma)$

Posterior mean and 95% credible intervals are obtained from 2,500 posterior draws. Least squares estimates are provided for comparison.

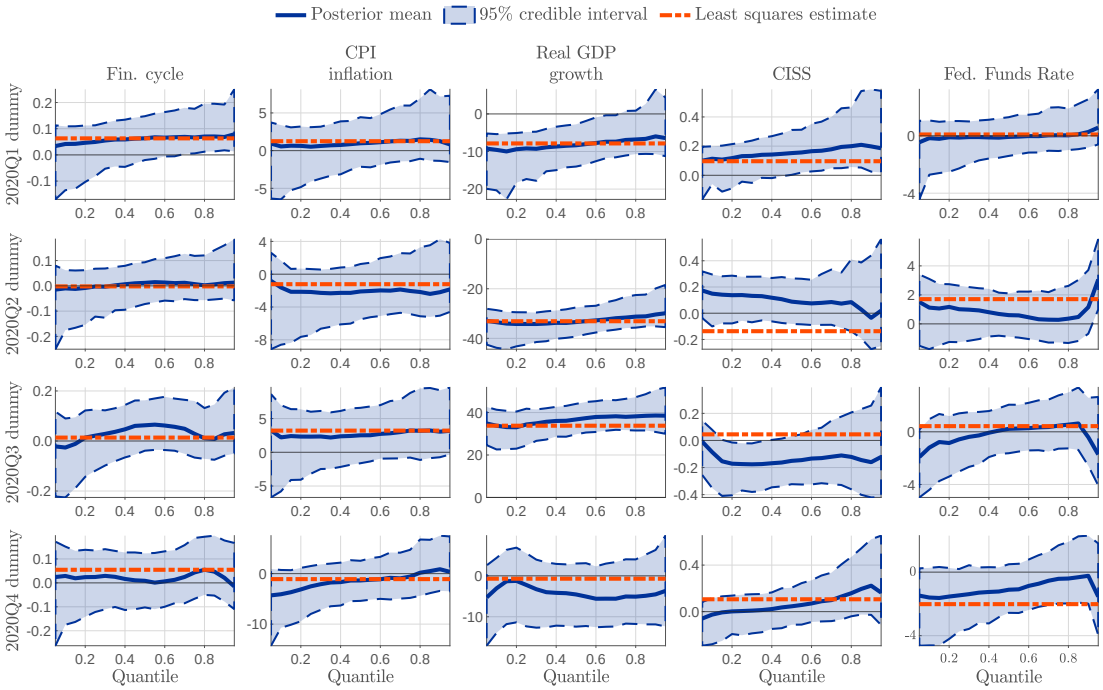

Figure E.9: Posterior mean estimates for U.S. prior tightness parameter $\lambda_i(\gamma)$

Posterior mean estimates of $\lambda_i(\gamma)$ are obtained from 2,500 posterior draws.

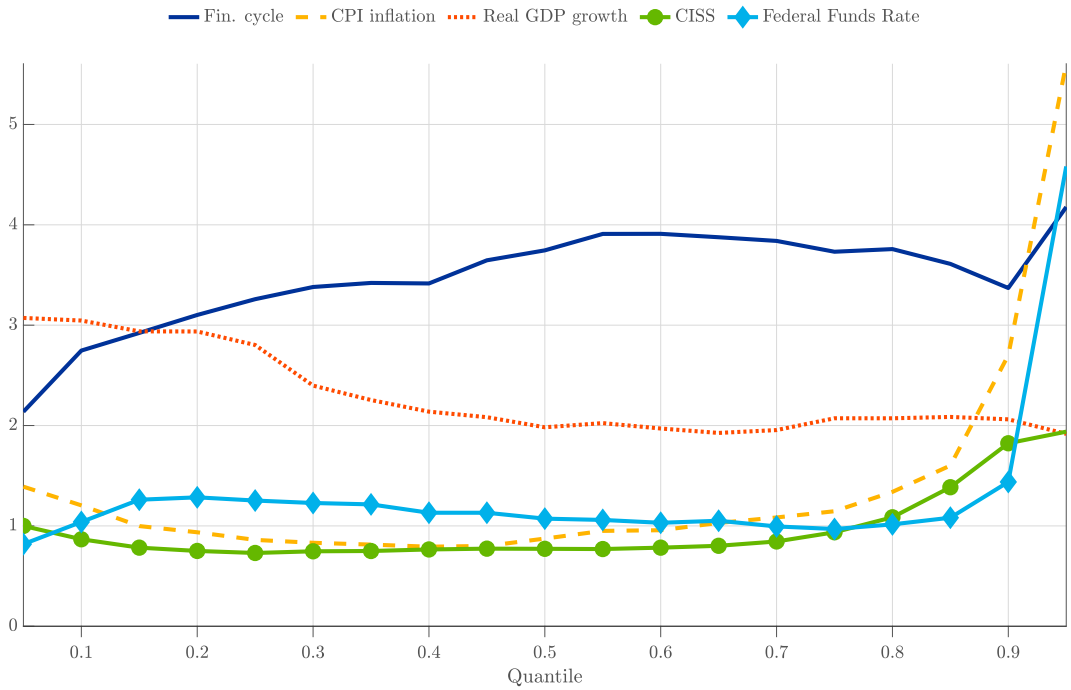

Figure E.10: Quantile impulse response functions for the U.S.

Impulse response functions implied by the posterior estimates reported in Figures E.1-E.8. Based on 400 draws from the posterior distribution and 20.000 forward simulations of the conditional distribution for each draw. Shocks are equal to the standard deviation of residuals from the median quantile regression of the respective variables. Variables are ordered financial cycle (respective first row), CPI inflation (second row), GDP growth (third row), CISS (fourth row), and the Federal funds rate (fifth row). Credible intervals are dashed and at a 95% level. Estimation sample is 1973Q1 to 2022Q4.

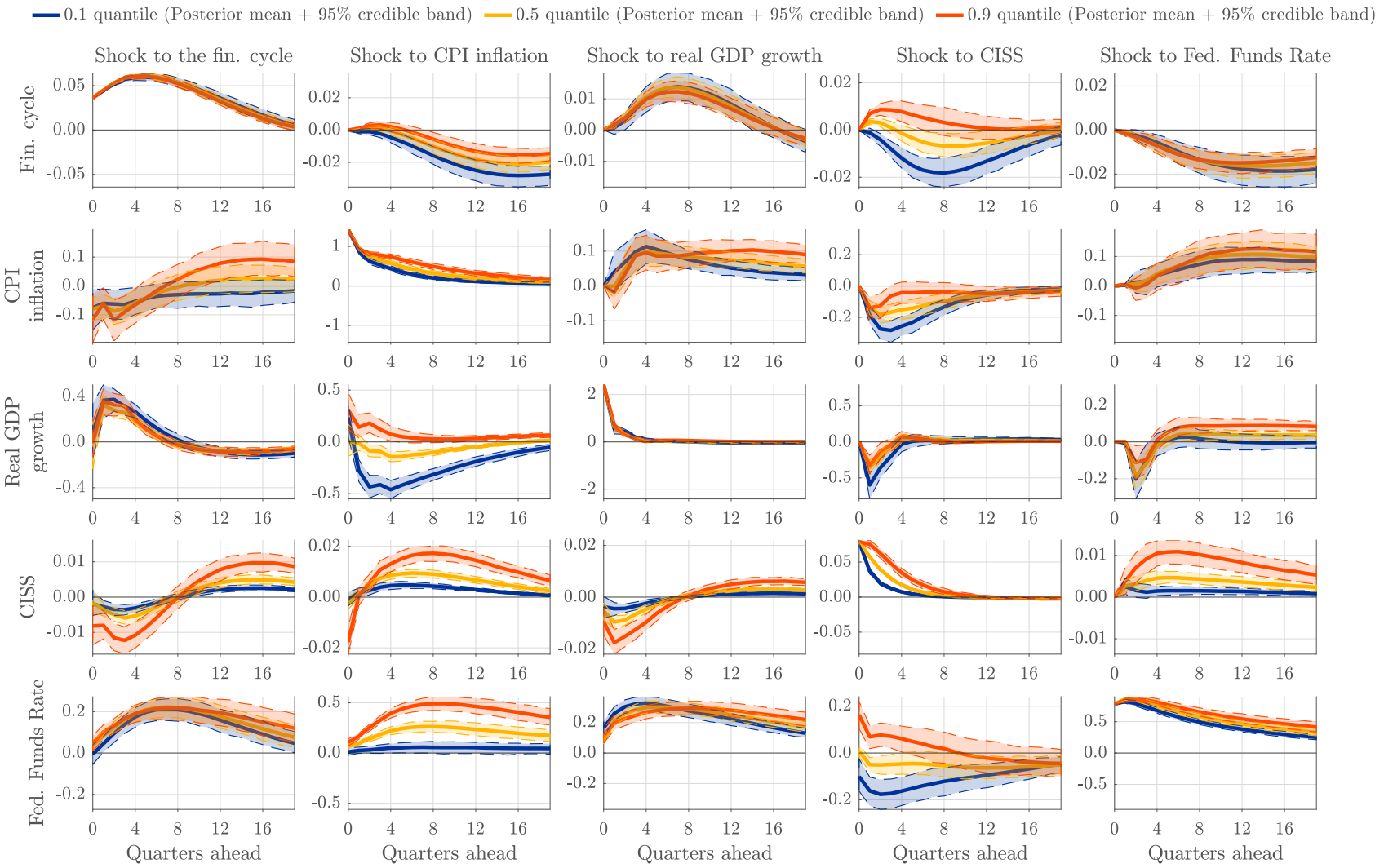

References

Chavleishvili, S. and S. Manganelli (2023). Forecasting and stress testing with quantile vector autoregression. *Journal of Applied Econometrics, forthcoming*.

Engle, R. F. and S. Manganelli (2004). CAViaR: Conditional autoregressive value at risk by regression quantiles. *Journal of Business & Economic Statistics 22*(4), 367–381.

Giannone, D., M. Lenza, and G. E. Primiceri (2015). Prior selection for vector autoregression. *The Review of Economics and Statistics 97*(2), 436–451.

Huber, F. and M. Feldkircher (2019). Adaptive shrinkage in bayesian vector autoregressive models. *Journal of Business & Economic Statistics 37*(1), 27–39.

Ibrahim, J. G. and M.-H. Chen (2000). Power prior distributions for regression models. *Statistical Science 15*(1), 46–60.

Ibrahim, J. G., M.-H. Chen, Y. Gwon, and F. Chen (2015). The power prior: Theory and applications. *Statistics in Medicine 34*(28), 3724–3749.

Khare, K. and J. P. Hobert (2012). Geometric ergodicity of the Gibbs sampler for Bayesian quantile regression. *Journal of Multivariate Analysis 112*, 108–116.

Koenker, R. and G. Bassett Jr (1978). Regression quantiles. *Econometrica 46*(1), 33–50.

Korobilis, D. (2017). Quantile regression forecasts of inflation under model uncertainty. *International Journal of Forecasting 23*, 11 – 20.

Korobilis, D. and D. Pettenuzzo (2019). Adaptive hierarchical priors for high-dimenstional vector autoregressions. *Journal of Econometrics 212*(1), 241–271.

Kozumi, H. and G. Kobayashi (2011). Gibbs sampling methods for Bayesian quantile regression. *Journal of Statistical Computation and Simulation 81*(11), 1565–1578.

Litterman, R. B. (1986). Forecasting with Bayesian vector autoregressions - five years of experience. *Journal of Business & Economic Statistics 4*, 25–38.

Luetkepohl, H. (2005). *New introduction to multiple time series analysis*. Springer, Germany.

Yu, K. and R. A. Moyeed (2001). Bayesian quantile regression. *Statistics & Probability Letters 54*, 437–447.